Food and Chemical Toxicology 160 (2022) 112798

Contents lists available at ScienceDirect

Food and Chemical Toxicology

journal homepage: www.elsevier.com/locate/foodchemtox

In vitro and *in vivo* evaluation of AFB1 and OTA-toxicity through immunofluorescence and flow cytometry techniques: A systematic review

Massimo Frangiamone [1], Alessandra Cimbalo [1], Manuel Alonso-Garrido, Pilar Vila-Donat [*], Lara Manyes

Laboratory of Food Chemistry and Toxicology, Faculty of Pharmacy, University of Valencia, Av. Vicent Andrés Estellés s/n, 46100, Burjassot, Spain

ARTICLE INFO

Handling Editor: Dr. Jose Luis Domingo

Keywords:
Mycotoxins
Toxicological mechanism
Cell line
Animal model
Organ

ABSTRACT

Due to the globalization, mycotoxins have been considered a major risk to human health being the main contaminants of foodstuffs. Among them, AFB1 and OTA are the most toxic and studied. Therefore, the goal of this review is to deepen the knowledge about the toxicological effects that AFB1 and OTA can induce on human health by using flow cytometry and immunofluorescence techniques *in vitro* and *in vivo* models. The examination of the selected reports shows that the majority of them are focused on immunotoxicity while the rest are concerned about nephrotoxicity, hepatotoxicity, gastrointestinal toxicity, neurotoxicity, embryotoxicity, reproductive system, breast, esophageal and lung toxicity. In relation to immunofluorescence analysis, biological processes related to AFB1- and OTA-toxicity were evaluated such as inflammation, neuronal differentiation, DNA damage, oxidative stress and cell death. In flow cytometry analysis, a wide range of assays have been performed across the reviewed studies being apoptosis assay, cell cycle analysis and intracellular ROS measurement the most employed.

Although, the toxic effects of AFB1 and OTA have been reported, further research is needed to clarify AFB1 and OTA-mechanism of action on human health.

1. Introduction

Mycotoxins are toxic secondary compounds synthesized under specific conditions by certain fungal species capable of growing in a wide variety of foodstuffs (Luo et al., 2018). Although more than 400 fungal metabolites with toxigenic potential have been reported, the most common and studied mycotoxins are aflatoxins (AFs), among them aflatoxin B1 (AFB1); ochratoxin A (OTA); citrinin; patulin; trichothecenes: deoxynivalenol (DON), T2 and HT2 toxin; fumonisins; zearalenone (ZEA) and emerging mycotoxins: fusaproliferin, moniliformin, beauvericin and enniatins (Khaneghah et al., 2019). These metabolites are mainly produced by fungi of the genera *Aspergillus, Fusarium, Penicillium and Alternaria* (Anfossi et al., 2016; Topi et al., 2021).

The growth of toxigenic fungi and mycotoxin production are widely dependent on environmental factors such as microbial competition, water activity (a_w), pH and oxygen concentration, temperature and relative humidity, which represent the driving force of fungal colonization (Mshelia et al., 2020). The Food and Agriculture Organization (FAO) estimates that approximately 25% of cereals produced in the world are contaminated by mycotoxins (FAO, 2013). However, other authors reported that 72–79% of feed samples from different part of the world contained mycotoxins, confirming a worldwide spreading (Streit et al., 2013; Kovalsky et al., 2016; Eskola et al., 2020). These toxic chemical compounds can be commonly found in processed and unprocessed foods: cereals, fruits, spices, coffee, milk, cheese, beer, wine, bread, chocolate and baby foods (Ayofemi Olalekan Adeyeye, 2020; Sarmast et al., 2020).

Due to their toxicological effects, mycotoxins can induce adverse effects on human and animal health even at low concentrations (Bryła et al., 2018). Once ingested, mycotoxins may cause acute or chronic disease: a) acute episodes are characterized by a rapid onset with an obvious toxic response including abdominal pain, coma, convulsions, pulmonary and cerebral edema and death; b) low-dose chronic exposures to mycotoxins over a long period of time reported toxic responses, including cancer, hepatic diseases, immune and neurological disorders

* **Corresponding author.** Laboratory of Food Chemistry and Toxicology, Faculty of Pharmacy, University of Valencia, Av. Vicent Andrés Estellés s/n, Valencia, 46100, Spain.
E-mail address: pilar.vila@uv.es (P. Vila-Donat).
[1] Both authors contributed equally to the manuscript.

https://doi.org/10.1016/j.fct.2021.112798
Received 8 October 2021; Received in revised form 3 December 2021; Accepted 24 December 2021
Available online 30 December 2021

Abbreviations

α-SMA	Alpha Smooth Muscle Actin
3D4/21	Continuous porcine cell lines from alveolar macrophages
8OHdG	8-hydroxiguanosine: 8-oxyguanine: 8-oxoG
A459	Adeno-carcinomic human alveolar basal epithelial cell line
AKT	Protein-kinase B
Arg-1	Arginase 1
ATP	Adenosine triphosphate
ATR	ataxia telangiectasia and Rad3-related
a_w	water activity
BRCA1	Breast cancer 1 susceptibility protein
BRL	Buffalo rat liver cell line
Caco-2	Human colorectal adenocarcinoma cell line
CD20	Cluster differentiation 20
CD45	Cluster differentiation 45
CMT93-II	Mouse rectum carcinoma cell line
CRM1	Chromosomal Maintenance 1
Dcx	Doublecortin
DNA	Deoxyribonucleic acid
DNMT1	DNA Methyltransferase 1
EBNA-2	The Epstein-Barr virus nuclear antigen 2
eDNA	Extracellular DNA
ER	Endoplasmic Reticulum
ET	Extracellular Traps
ERK1/2	Extracellular signal-regulated protein kinases 1 and 2
F2R	Coagulation factor II thrombin receptor
GC-2	Germ cell line
Ges-1	Human gastric epithelial cell line
GFAP	Glial Fibrillary acidic protein
Gpx	Glutathione peroxidase
GSDMD	Gasdermin D
H3K9ac	Recombinant Histone H3 acetyl Lys9
H3K9me3	Recombinant Histone H3 trimethyl Lys9
H9-T	Human cutaneous $CD4^+$ T lymphoma cell line
HCT-116	Human colon carcinoma cell line
HCT-8	Human ileocecal adenocarcinoma cell line
HEK293T	Human embryonic kidney 293 cell line
HepaRG	Differentiated hepatic cell line
HepG2	Human liver cancer cell line
HET-1A	Human esophageal epithelial cell line
HIF-1α	Hypoxia inducible Factor 1
HK-2	Human renal proximal tubule epithelial cell line
HKC cells	Human proximal tubular epithelial cell line
HO-1	Heme oxygenase
Iba1	Ionized calcium binding adaptor molecule 1
iNOS	Inducible Nitric Oxide Synthase
IPECJ2	Intestinal Porcine Epithelial cell line-J2
ITGB1	Integrin beta 1
Kim-1	Kidney injury molecule-1
L02	Human fetal hepatocyte
LX-2	Human hepatic stellate cell line
MAP2-AP18/M13	Microtubule-Associated Protein 2 clone AP18 and M13
MDCCs	monocyte-derived dendritic cells
MDCK cells	Madin-Darby Canine Kidney cell line
mGalc	Galactocerebroside
MPO	Myeloperoxidase
NAC	N-acetylcysteine
NADP	Nicotinamide adenine dinucleotide phosphate
NeuN	Neuronal nuclei
NF-kB	Nuclear factor kappa-light-chain-enhancer of activated B cells
NLRP3	NLR family pyrin domain containing protein 3
NP	Nucleoprotein
NRF2	The nuclear factor erythroid 2-related factor 2
NRK-52E	Normal rat kidney cells clone 52E
p65	Nuclear factor NF-kappa-B p65 subunit
PCNA	Proliferating cell nuclear antigen
PI	propidium iodide
PI3K	Phosphatidyl-Inositol 3-Kinase
PK15	Porcine kidney 15 cell line
PTEN	Phosphatase and tensin homolog
Rad51	DNA repair protein RAD51 homolog 1
RAW 264.7	Mouse leukemic monocyte-macrophage cell line
RIP3	Receptor-interacting serine/threonine-protein kinase 3
RNA	Ribonucleic acid
SOD	Superoxide dismutase
TM3-TM4 cell line	Mouse Leydig and Sertoli cell line
TNF	Tumor Necrosis Factor
t-RNA	RNA transfer
TOM20	Mitochondrial import receptor subunit TOM20 homolog
Zo1	Tight junction protein-1
γH2A	Trypanosomal histone γH2A

(Alshannaq and Yu, 2017). It should be emphasized that not all mycotoxins exhibit the same toxicity as their detrimental effects depend on the characteristics (age, nutrition, metabolism and other factors as well) of humans and animals affected (Bertero et al., 2018; Cimbalo et al., 2020).

Consequently, the International Agency for Research on Cancer (IARC) has classified mycotoxins into five groups (Group 1, 2A, 2B, 3 and 4) according to their carcinogenicity (IARC, 2012). Nevertheless, due to their widespread occurrence and well-known toxicity, AFB1 and OTA are to be considered with a major caution (Kutsanedzie et al., 2020). Table 1 shows their fungal producing species, maximum tolerable levels, contaminated foods, affected organs, toxicological mechanisms and damages.

1.1. Aflatoxins

AFs are the most toxic mycotoxins for human health (Singh et al., 2021). They are polypeptide compounds produced by many species of *Aspergillus*, mainly by *Aspergillus flavus* and *Aspergillus parasiticus* (Kumar et al., 2017). The most important factors in fungi colonization and toxin production are temperature and a_w. In particular, optimum temperature and a_w values are ranged between 16 and 31 °C and 0.82–0.99 a_w (Bernáldez et al., 2017; Sarma et al., 2017). AFs production occurs in a wide range of food commodities: cereals, spices, tree nuts, milk and dried fruits (Umesha et al., 2017).

Several studies have shown that AFs contamination induce mutagenicity, hepatotoxicity, immunotoxicity and carcinogenicity (Ostry et al., 2017; Rushing and Selim, 2019). Therefore, they are classified by IARC in group 1 as carcinogenic to humans (IARC, 2012). In order to protect human health, it is essential to keep these food contaminants at toxicologically acceptable levels. The European Union (EU) sets the maximum tolerable limits of AFB1 at 2–5 μg/kg in cereals, 2–8 μg/kg in dried fruits, 5 μg/kg in spices, 6 μg/kg in dietary foods for medical purpose and 0.1 μg/kg in foods for infants and young children (EC European Commission, 2006).

Mechanistically, AFB1-exo isomer 8,9-epoxide (AFBO), formed in the first step of AFB1 metabolism, has been considered as the major responsible for their genotoxicity. AFBO reacts with DNA, RNA and proteins forming the toxic adduct 8,9-dihydro-8(N7-guanyl)-9-hydroxy-AFB1 (AFB1–N7-Gua), which confers mutagenic properties (Dai et al.,

Table 1
AFB1 and OTA fungi producers, maximum tolerable levels, foodstuffs, organ affected, toxicological mechanism, damage and references.

MYCOTOXINS	FUNGI PRODUCERS	MAXIMUM TOLERABLE LEVELS	FOODSTUFFS	ORGAN AFFECTED	TOXICOLOGICAL MECHANISM	DAMAGE	REFERENCES
Aflatoxin B1	*Aspergillus (Flavius and parasiticus).*	Dried fruits 2–8 μg/kg, cereals 2–5 μg/kg, spices 5 μg/kg, baby foods 0.1 μg/kg.	Cereals, oil seeds, spices, tree nuts, milk, meat and dried fruits.	Liver, Immune system	Adducts formation with DNA and proteins. Lipid peroxidation, oxidative stress and apoptosis.	Mutagenicity, hepatotoxicity, immunotoxicity, carcinogenicity, neurotoxicity.	Ráduly et al. (2020) Rushing & Selim (2019) Niaz et al. (2020) EC Commission (2006)
Ochratoxin A	*Aspergillus (alliaceus, auricomus, carbonarius, cretensis, flocculosus, glaucus, lacticoffeatus, meleus, niger, ochraceus, pseudoelegans, roseoglobulosum, sclerotioniger) Penicillium (nordicum, verrucosum).*	Soluble coffee 10 μg/kg, unprocessed cereals 5 μg/kg, fruit juice and wine 2 μg/kg, spices 15 μg/kg, dietary and baby foods 0.5 μg/kg.	Cereals, wine, tea, coffee, milk, cheese, meat, fish, eggs, fruits, dried fruits, spices and vegetables.	Liver, kidney.	Inhibition of ATP production. Lipid peroxidation and ROS generation and apoptosis.	Nephrotoxicity, hepatotoxicity, immunotoxicity, neurotoxicity.	Zhao et al. (2017) Chen et al. (2018) Ráduly et al. (2020) EC Commission (2006)

2017; Benkerroum, 2020).

In view of this, AFB1-exposure may induce severe implications on the immune system, liver, epididymis, kidney and heart (Xu et al., 2020). Likewise, the high lipid solubility of AFB1 and its existence in the *post mortem* brain tissue (Bahey et al., 2015) suggest its ability to cross the blood brain barrier (BBB), thus affecting its integrity (Qureshi et al., 2015). In the central nervous system (CNS), AFB1 may disturb neural cell functions by forming DNA and protein adducts and by inducing oxidative stress, apoptosis and the inhibition of macromolecules synthesis (Alsayyah et al., 2019).

1.2. Ochratoxins

Ochratoxins are the most common mycotoxins detected in foodstuffs (Malir et al., 2016). There are 3 groups: Ochratoxin A (OTA), B (OTB), C (OTC), which are produced by different species of *Aspergillus* and *Penicillium* (Heussner and Bingle, 2015). Among these, OTA, an organic toxin with low molecular weight, is the most abundant and detrimental (Kőszegi and Poór, 2016). Optimum temperature and a_w values for mycotoxin production are ranged between 15 and 25 °C and 0.90–0.99 a_w (Sánchez-Montero et al., 2019). Typical contaminated foods are cereals (maize, wheat, rice, sorghum, barley, oats) cereal-based products (bread, flour, and pasta), wine, tea, coffee, milk, cheese, dried fruits, spices and vegetables (Chen et al., 2018).

OTA has been classified by IARC in group 2B as possible carcinogen for human (IARC, 2012). The EU sets the maximum permissible levels of OTA in unprocessed cereals at 5 μg/kg, 8 μg/kg in wheat gluten, in roasted coffee beans at 5 μg/kg and 10 μg/kg in soluble coffee, 15 μg/kg in spices, 2 μg/kg in grape juice and wine, in liquorice between 20 and 80 μg/kg, in baby foods and dietary foods for medical purpose at 0.5 μg/kg (EC European Commission, 2006).

Mechanistically, OTA exerts its toxicity by increasing NADPH and P450 enzyme activity, or by promoting caspase signaling pathway and apoptosis. In addition, OTA may elicit oxidative stress in mitochondria and alter cell cycle, lipid and nucleotide metabolism (Zhu et al., 2017; Tao et al., 2018).

Consequently, OTA-exposure determinate various toxicological effects, including the disruption of gut microbiota homeostasis, hepatotoxicity, genotoxicity, immunotoxicity, embryotoxicity, neurotoxicity, testicular toxicity and nephrotoxicity (Luz et al., 2018; Leitão, 2019). Despite limited evidences, the association between OTA-exposure with Balkan Endemic Nephropathy, Chronic Interstitial Nephropathy and other kidney diseases has been demonstrated (Zhao et al., 2017). Furthermore, *in vivo* studies suggest that OTA crosses the BBB and accumulates in cerebellum, ventral mesencephalon, striatum, pons and cerebral cortex (Niaz et al., 2020). High doses of OTA have been also found in hippocampus, the primary site of neurodegeneration in Alzheimer disease (Bhat et al., 2016). In brain, OTA triggers reactive oxygen species (ROS) generation, alterations in cell cycle and proteome profiles, caspase activation and disruption of mitochondrial membrane potential (MMP) (Park et al., 2019; Babayan et al., 2020).

Nowadays, several molecular techniques can be employed to determinate the toxicological mode of action (MOA) of mycotoxins in organisms. Naturally, the main tool used are -omics techniques, which allow to analyze both *in vivo* and *in vitro* systemic changes induced by harmful compounds (Soler and Oswald, 2018; Cimbalo et al., 2020). In addition, flow cytometry (FCM) and microscopy can be excellent tools for studying mycotoxin toxicity. FCM is an automated and high throughput method which allows a very rapid analysis of multiple chemical and physical characteristics of single cells. It is an extremely useful technology which has been used for decades with filamentous fungi (Bleichrodt and Read, 2019). Furthermore, FCM provides an excellent interpretation of cellular processes such as redox balance, proliferation and apoptosis (Zhou et al., 2020; Broemsen et al., 2021). Whilst, microscopy, which is a rapid, cheap and simple technic, allows to investigate and examine histological changes on tissues induced by mycotoxins and through specific antibodies and fluorescence kits it enables to analyze their specific MOA (Nguyen et al., 2019; Gémes et al., 2021).

Therefore, the goal of this review is to deepen the knowledge about AFB1 and OTA toxicity *in vitro* and *in vivo* models by using FCM and immunofluorescence (IF) techniques.

2. Material and methods

An extensive bibliographic research was conducted using four different scientific databases: PubMed, Web of science, Scopus and Google scholar by selecting articles in the last six years (2015–2021). The research was carried out by using the following keywords: AFB1, OTA, microscopy and flow cytometry. To facilitate the screening in google scholar, which covers the same importance of other scientific databases in bibliographic research but includes a less quality publications from some websites (Kousha and Thelwall, 2008; Martín-Martín et al., 2021), the research was refined by using the terms: immunofluorescence, *in vivo, in vitro,* mycotoxins, mechanism, toxicity, biological effects and toxicological damage. A number of 733 articles, which met the criteria to be included into the study, were analyzed. Reports obtained were assessed by screening abstract to discard unnecessary,

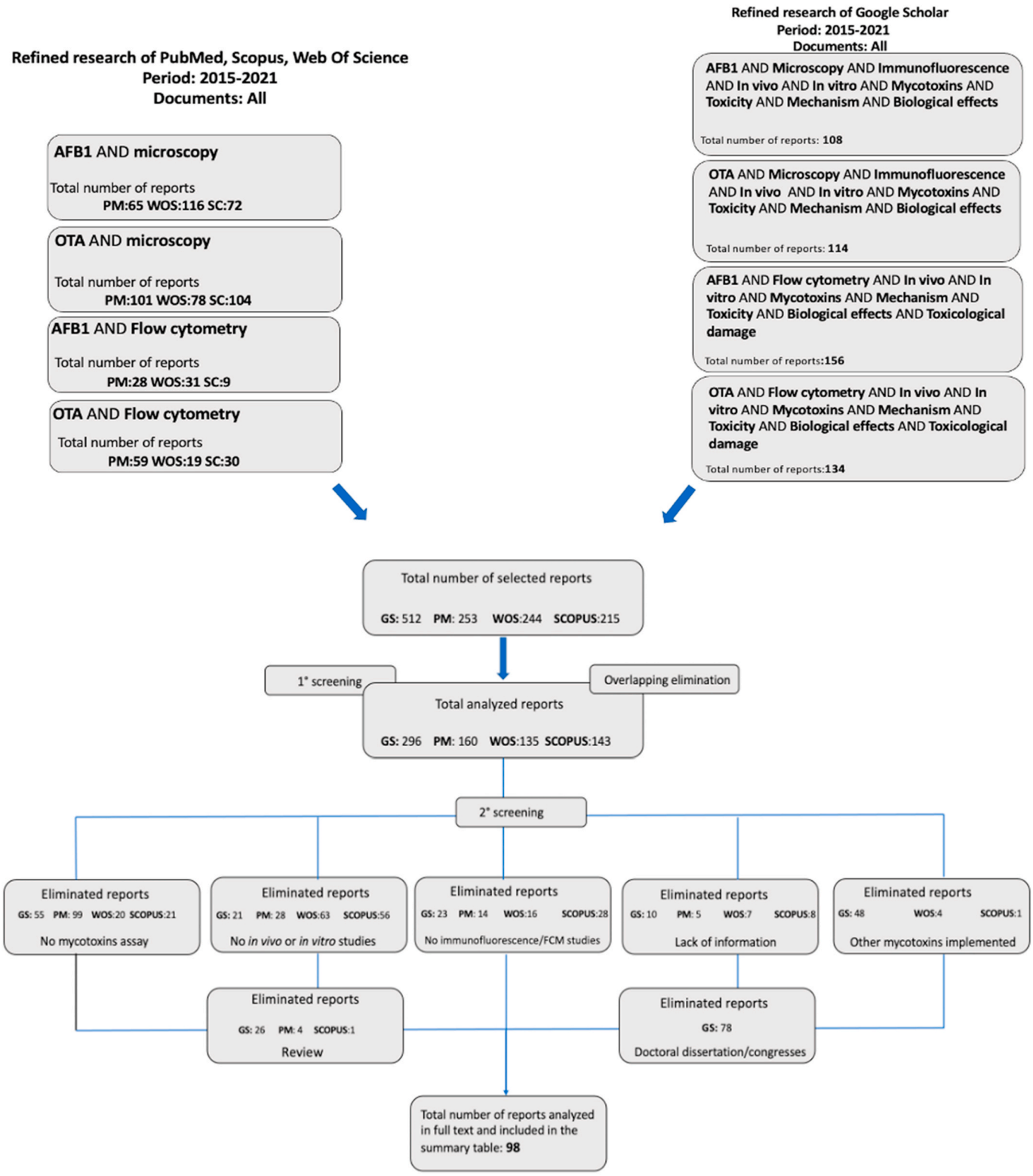

Fig. 1. Graphic representation of total number of articles screened throughout the bibliographic research.

incomplete or irrelevant literature. Finally, a total of 98 articles were analyzed in full text and classified based on: type of mycotoxin, technique used, analysis model (*in vitro* or *in vivo*), dose administration, exposure time, antibodies implemented or FCM assays and toxicological mechanism (Fig. 1).

3. Results

3.1. Aflatoxin B1

AFB1 is the best known and most studied mycotoxin. In this review, its toxicity was elucidated through IF and FCM techniques. Regarding IF analysis, antibodies varied depending on the specific mechanism or

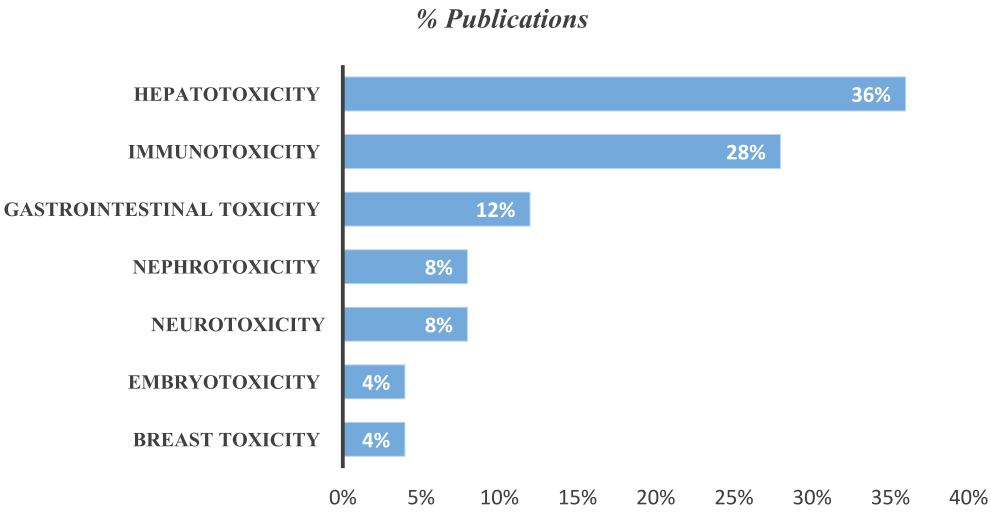

Fig. 2. Percentage of total publications (n = 25) according to the main toxicological effects of AFB1 *in vitro*.

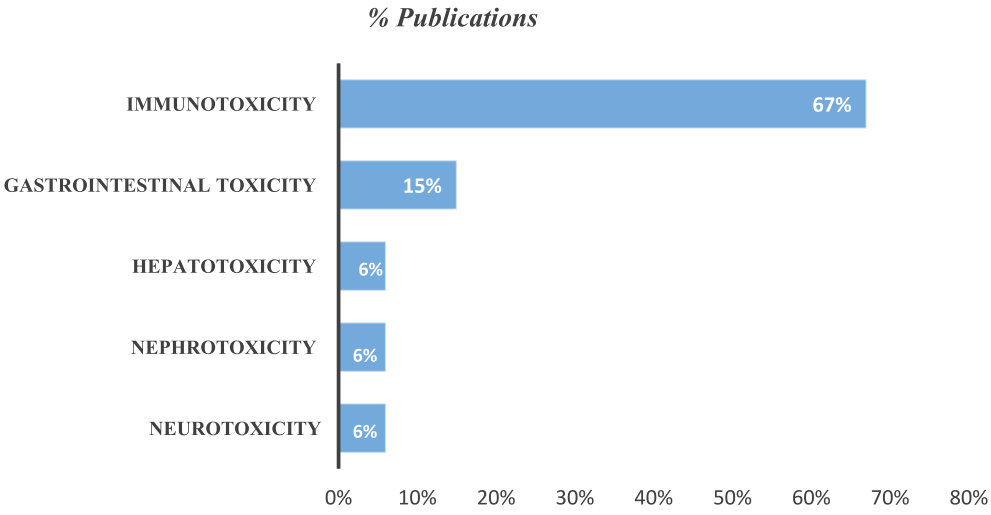

Fig. 3. Percentage of total publications (n = 20) according to the main toxicological effects of AFB1 *in vivo*.

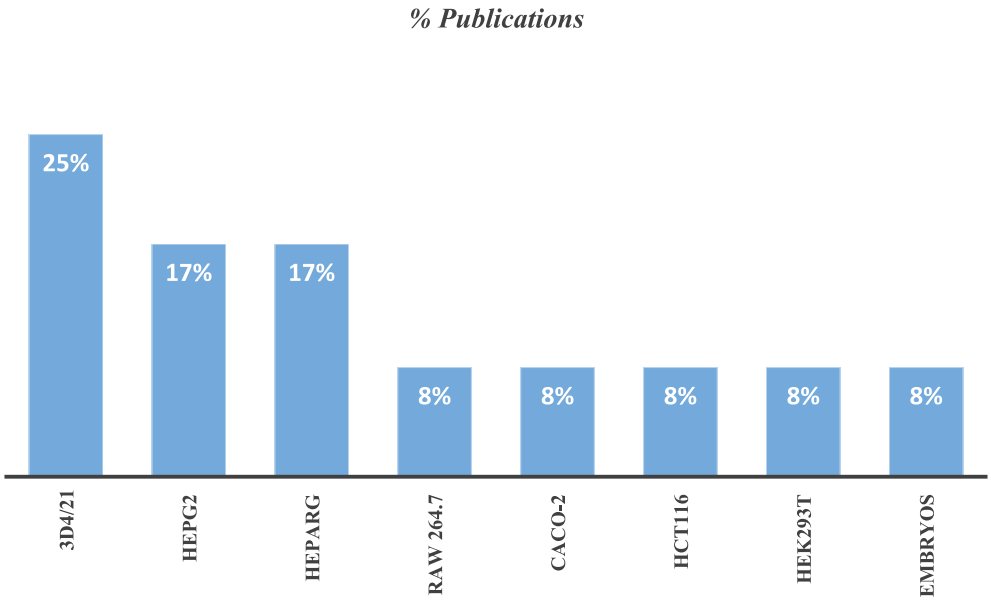

Fig. 4. Percentage of publications (n = 10) according to cell lines used in AFB1-IF *in vitro* studies.

Table 2
AFB1-IF studies: *In vitro* and *in vivo* model, dose and exposure time, antibodies implemented, mechanism and references.

In vitro/in vivo model	Dose administration	Exposure time	Antibodies used	Mechanism	References
In vitro Immunotoxicity					
RAW264.7 cells	0.62 μg/ml	2 h	Anti-iNOS, anti-Arg-1, anti-MPO, anti-elastase, anti-eDNA, anti-histone H3	Induction of ROS-Mediated Autophagy and Extracellular Trap Formation.	An et al. (2017)
3D4/21 cells	1×10^{-2}, 2×10^{-2}, 4×10^{-2} μg/ml	24 h	Anti-NP	Promotion of Swine influenza virus.	Sun et al. (2018)
3D4/21 cells	2×10^{-2}, 4×10^{-2}, 8×10^{-2}, 0.16 μg/ml	48 h	Anti-γH2AX	Apoptosis, ROS generation and DNA damage with epigenetic modifications.	Zhou et al. (2019)
3D4/21 cells	0.16 μg/mL + NAC (652 μg/ml)	48 h	Anti-p65, anti-NF-kB	Activation of NF-κB pathway and promotion of apoptosis, inflammation and oxidative stress.	Hou et al. (2018)
Hepatotoxicity					
HepG2 cells	10 μg/mL + $ZnSO_4$ (8.1 μg/ml) or $ZnSO_4$ (4 μg/ml) + GZn (11.4 μg/mL)	24 h	Anti-AFB1	Promotion of ROS generation, cell cycle arrest and apoptotic bodies formation. Induction of DNA strand breaks and epigenetic changes.	Yang et al. (2016)
HepaRG cells	0.31 μg/ml	24 h	Anti-GSDMD	Promotion of hepatocytes pyroptosis and activation of Kupffer cells with liver inflammatory.	Zhang et al. (2019)
HepG2 cells HepaRG cells	0.31 μg//ml	48–72 h	Anti-TOM20, anti-RIP3	Induction of Hepatitis B virus infection, hepatic steatosis and mitochondrial disorders.	Chen et al. (2019)
Gastrointestinal toxicity					
HCT116 cells Caco-2 cells	3.12 μg//ml	8 h	Anti-yH2AX, anti-p53BP1	Enhancement of cell death and DNA damage-mediated cell cycle arrest through the ATR-Chk1 axis.	Gauthier et al. (2020)
Nephrotoxicity					
HEK293T cells	1, 2, 6 μg/ml	24 h	Anti-CRM1	Cell cycle arrest.	Huang et al. (2019)
Embryotoxicity					
Porcine embryos	3.12×10^{-4} μg/ml	1 week	Anti-LC3, anti-cytochrome C, anti-53BP1, anti-γH2AX, anti-BECLIN1	Disturbance of embryonic development, production of ROS and DNA damage. Induction of apoptosis and autophagy with a reduction of cell proliferation.	Shin et al. (2018)
In vivo Neurotoxicity					
Rats brain	0.016 mg/kg/orally	8 weeks	Anti-NeuN, anti-GFAP	Structural alterations in rat brain with an increase of astrocyte distribution and a reduction of neuronal cells.	Bahey et al. (2015)
Immunotoxicity					
Mice spleen	0.05–0.07 mg/kg/ intraperitoneally	8–10 weeks	Anti-EBNA2, anti-CD20	Promotion of EBV carcinogenesis.	Accardi et al. (2015)

metabolic route searched by authors. FCM was mainly used to detect alterations in cell cycle, mitochondrial balance, ROS generation and apoptosis/necrosis induction. Interestingly, FCM was also employed to quantify and identify particular markers, apoptotic DNA and cell subsets. Furthermore, several natural compounds, food components and non-pathogenic bacteria have been employed to ameliorate AFB1-toxicity such as: β-1,3-glucan, zinc sulfate ($ZnSO_4$) gluconate (GZn) and bentonite (Zn-Bent1), L-proline, selenium (Se), palm kernel cake (PKC), gallic acid, N-acetylcysteine (NAC), *Lactobacillus paracasei* (LP) BEJ01, montmorillonite clay (MT), egg yolk immunoglobulin (IgY) and lactic acid bacteria (LAB).

For each technique, the selected AFB1-studies were organized according to the model used (*in vitro* and *in vivo)*, showing that the main AFB1-toxicological effects *in vitro* are hepatotoxicity, immunotoxicity, gastrointestinal toxicity, nephrotoxicity, neurotoxicity, embryotoxicity and breast toxicity (Fig. 2). Whilst, immunotoxicity, gastrointestinal toxicity, hepatotoxicity, nephrotoxicity and neurotoxicity were mainly observed *in vivo* (Fig. 3). The summary of the studies found for AFB1 are shown below. Tables were divided according to the technique, model used and type of toxicity, and were ordered by the exposure time, from the shortest to the longest.

3.1.1. Immunofluorescence

3.1.1.1. In vitro toxicity. *In vitro* AFB1-IF studies show exposure times between 2 h and 7 days and concentrations of 3.12×10^{-4}-10 μg AFB1/ml. As shown in Fig. 4, the most used cell line was 3D4/21. The natural compounds implemented to reduce AFB1-damages were zinc, sulfate and gluconate, and NAC.

3.1.1.1.1. Immunotoxicity. In the shortest exposure, AFB1 triggered an immune and pro-inflammatory response in macrophages through ROS-mediated autophagy and extracellular traps (ETs) production. The major components of ETs, elastase, myeloperoxidase, and histone H3, were disrupted by toxin exposure. In addition, by the analysis of typical markers of macrophage polarization, it has been observed a M1 polarization of macrophages, which acquired pro-inflammatory properties (An et al., 2017).

Furthermore, acute exposure to AFB1 exacerbated swine influenza virus (SIV) infection, inflammation and lung damage by activating TLR4-NFκB signaling pathway. In contrast, TAK242 and TLR4 knockout, TLR4-specific antagonist, alleviated the AFB1-promoted SIV replication, inflammation and lung damage (Sun et al., 2018). In a similar duration study, AFB1 induced oxidative stress, cell death and the production of pro-inflammatory cytokines. It also caused genomic damages, identified by γH2AX fluorescent analysis, a specific histone wrapping around DNA.

Table 3
AFB1-FCM studies: *In vitro* model, dose and exposure time, FCM assay, mechanism and references.

In vitro model	Dose administration	Exposure time	FCM assay	Mechanism	References
Immunotoxicity					
RAW264.7 cells	7.7×10^{-2} - 0.62 μg/ml	1.5 h	Macrophages subset analysis	Induction of ROS-Mediated Autophagy and Extracellular Trap Formation.	An et al. (2017)
MDDCs cells	1×10^{-2} μg/ml	2–12 h	Apoptosis assay Phagocytosis assay	Impairment of cell phagocytosis activity and function. Increase of cell death.	Mehrzad et al. (2018)
Human, dog and cattle leukocytes	1×10^{-2} μg/ml	24 h	Apoptosis assay	Depletion of intracellular ATP and apoptosis.	Mehrzad et al. (2020)
Human lymphocytes	0.2, 2, 20 μg/ml	24 h	DNA damage analysis	Promotion of oxidative stress by inducing lipid peroxidation.	Su et al. (2017)
3D4/21 cells	2×10^{-2}, 4×10^{-2}, 8×10^{-2}, 0.16 μg/ml	48 h	Analysis of immune cells subset Apoptosis assay	Promotion of Swine influenza virus.	Sun et al. (2018)
3D4/21 cells	2×10^{-2}, 4×10^{-2}, 8×10^{-2}, 0.16 μg/ml	48 h	Apoptosis assay	Apoptosis, ROS generation and DNA damage with epigenetic modifications.	Zhou et al. (2019)
3D4/21 cells	0.16 μg/ml	48 h	Apoptosis assay Intracellular ROS measurement	Activation of NF-κB pathway and promotion of apoptosis, inflammation and oxidative stress.	Hou et al. (2018)
Hepatotoxicity					
Broiler hepatocytes	0.15, 0.31, 0.77, 1.56 μg/ml	6 h	Apoptosis assay Measurement of mitochondrial membrane potential	Impairment of mitochondrial functions, ROS generation and induction of apoptosis.	Liu et al. (2016)
HepG2 cells	10 μg/mL + $ZnSO_4$ (8.1 μg/ml) or $ZnSO_4$ (4 μg/ml) + GZn (11.4 μg/ml)	24 h	Cell cycle analysis AFB1-DNA adduct formation	Promotion of ROS generation, cell cycle arrest and apoptotic bodies formation. Induction of DNA damages and epigenetic changes.	Yang et al. (2016)
HepG2 cells	0.62 μg/ml	24 h	Cell cycle analysis	Pathological impairment and cell cycle alteration.	(K. Chen et al., 2016)
HepG2 cells	3.12×10^{-3}, 1.88, 3.12 μg/ml	24, 48 h	Cell cycle analysis Apoptosis assay Measurement of mitochondrial membrane potential	Disturbance in cell cycle, promotion of apoptosis and ROS through mitochondrial impairments.	Du et al. (2017)
Chicken hepatocytes	1.56 μg/ml + Palm kernel cake (5, 10, 20, 40 μg/ml) + Acid gallic (1.7 μg/ml)	48 h	Apoptosis assay	Induction of lipid peroxidation and apoptosis.	(Oskoueian et al., 2015)
HepG2 cells	1.56, 3.12, 6.24 μg/ml	48 h	Quantitative determination of hepatocellular cancer stem cells	Promotion of hepatocellular carcinoma.	Ju et al. (2016)
L02 cells	31.2 μg/ml + IgY (9×10^{-2}, 4.7×10^{-2}, 2.3×10^{-2} μg/ml)	48 h	Cell cycle analysis Apoptosis assay AFB1-DNA adduct formation Intracellular ROS measurement	Apoptotic bodies formation and DNA strand breaks, with G_2/M phase cell cycle arrest. High ROS production with MPP disturbance.	Qiu et al. (2018)
Gastrointestinal toxicity					
HCT-8 cells	3.12 μg/ml	24 h	DNA apoptotic analysis	Promotion of DNA damage and cell cycle alteration via p53 activation. Possible cross-talk between AFB1 and OTA.	Kim et al. (2016)
Caco-2 cells	9.3 μg/mL + Zn-Bent1 (600 μg/ml)	48 h	Apoptosis assay	Promotion of necrosis.	Nones et al. (2017)
HCT116 cells Caco-2 cells	7.8×10^{-2}, 0.31,1.56, 3.12, 6.24 μg/ml	48 h	Apoptosis assay Cell cycle analysis Intracellular ROS measurement	Enhancement of cell death and DNA damage-mediated cell cycle arrest through ATR-Chk1 axis.	Gauthier et al. (2020)
Nephrotoxicity					
HEK293T cells	100 μg/ml + L-proline (1000 μg/ml)	24 h	Apoptosis assay	Disturbance in cell vitality.	Li et al. (2019)
HEK293T cells	1, 2, 6 μg/ml	24,48 h	Cell cycle analysis	Cell cycle arrest.	Huang et al. (2019)
Neurotoxicity					
Mouse astrocytes	1×10^{-1} μg/ml	24,48,72 h	Apoptosis assay	Apoptosis in a time dependent manner with intracellular ATP depletion and caspases 3–7 activation.	Vahidi-Ferdowsi et al. (2018)
Human microglia cells	2×10^{-2} μg/ml	48 h	Apoptosis assay	Apoptosis with intracellular ATP depletion and caspases 3–7 activation.	Mehrzad et al. (2018)
Breast toxicity					
BME cells	2 μg/ml	24 h	Cell cycle analysis Apoptosis assay Intracellular ROS measurement	Promotion of epigenetic modification in RNA-methylation. Impairment in cell cycle, proliferation and apoptosis.	Wu et al. (2021)

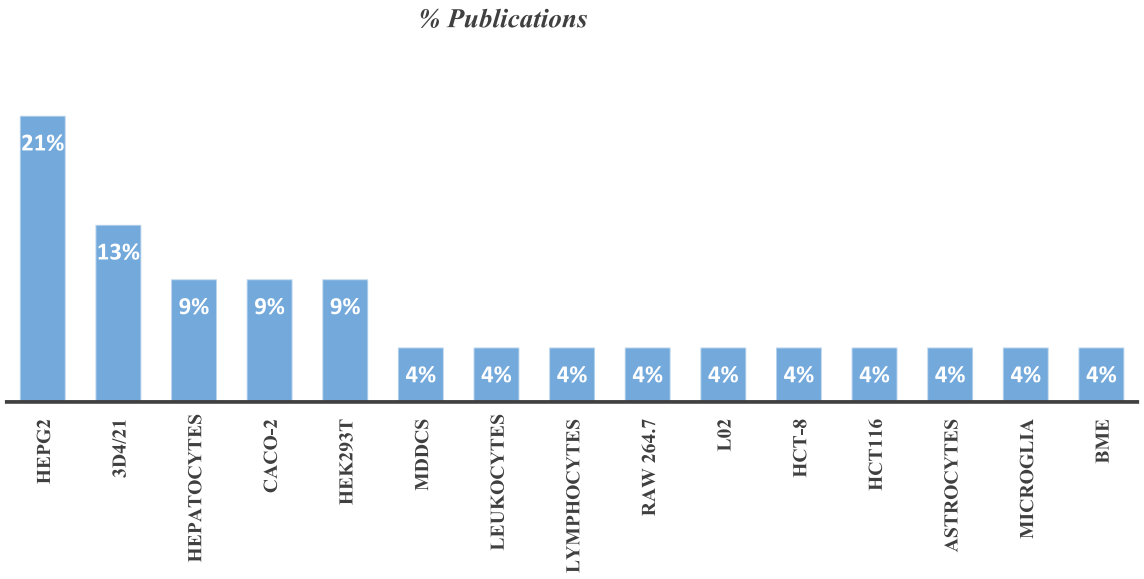

Fig. 5. Percentage of publications (n = 23) according to the cell lines used in AFB1-FCM *in vitro* studies.

Authors associated AFB1-immunotoxicity with JAK2/STAT3 pathway activation and the alteration of gene and protein expression of DNA methyl transferases 1 and 3a (Zhou et al., 2019).

In the 48 h study, AFB1 alone or in combination with OTA could aggravate immunotoxicity through the degradation of nuclear factor of kappa light polypeptide gene enhancer in B-cells inhibitor alpha (IκBa), the phosphorylation of nuclear factor kappa B, and its translocation into nuclei. Owing to AFB1-exposure, the expression of pro-inflammatory cytokines and ROS production were significantly increased. However, high doses of NAC and BAY11-7082, a specific inhibitor of NF-κB, suppressed oxidative stress, inflammation and immunotoxicity of both mycotoxins (Hou et al., 2018).

3.1.1.1.2. Hepatoxicity. As regards hepatotoxicity, AFB1 promoted nuclear changes with chromatin fracture-induced DNA double strand breaks (DSB) and oxidative DNA damage. However, $ZnSO_4$ and GZn reversed AFB1-promoted epigenetic changes and ameliorated cell survival, DNA integrity and the genome wide methylation (Yang et al., 2016). Zhang et al. (2019) demonstrated that exposure to toxin promoted the pyroptosis of hepatocytes via COX-2, inducing both NLRP3 and caspase 1 activation with IL-1β release. The fluorescent quantification of Gasdermin D, a novel regulator of caspase 1-mediated pyroptosis, confirmed its involvement in liver inflammation.

In the longest exposure, AFB1 enhanced Hepatitis B virus (HBx) infection in mutated liver cells. The combination of HBx and AFB1 exacerbated hepatic steatosis via COX-2 up-regulation and increased the expression of RIP3, a component of TNF receptor and strong inducer of apoptosis and inflammation. Additionally, AFB1 promoted mitochondrial disorders by altering TOMM20 expression, a central component in the recognition and translocation of mitochondrial proteins (Chen et al., 2019).

3.1.1.1.3. Gastrointestinal toxicity. As shown in Table 2, only one study about gastrointestinal toxicity was reported. In Caco-2 and HCT116 cells, AFB1 triggered cell death and DNA damage through ATR-Chk1 specific axis. The IF-analysis performed on γH2AX and p53, showed that ATR-axis was activated by replicative stress, a molecular and early response to AFB1, which subsequently led to DNA-DSB formation. In addition, an aberrant intracellular ROS generation (2-fold higher in comparison to the control) has been observed (Gauthier et al., 2020).

3.1.1.1.4. Nephrotoxicity. In kidney, the immunostaining of exportin 1, also known as CRM-1, showed that AFB1 increased significantly the nuclear volume inducing abnormal changes in DNA, such as polyploidy. CRM-1 mediates the nuclear proteins export playing a crucial role in cell cycle regulation, centrosome duplication and spindle assembly. Consequently, alterations in CRM-1 expression were closely related to cell cycle arrest and DNA damage (Huang et al., 2019).

3.1.1.1.5. Embryotoxicity. Toxicological damages were also detected in porcine embryos. In the longest exposure, 1 week, the lowest concentration of AFB1 reported (3.12×10^{-4}μg/ml) compromised embryonic development by the induction of oxidative stress and DNA damage, revealed by γH2AX fluorescence analysis. Moreover, AFB1 disrupted DNA damage mechanism repair through the dysregulation of p53 binding protein 1 and triggered autophagy, as shown by an overexpression of its typical markers, Beclin-1 and LC3. At the same time, the presence of AFB1 significantly impaired cell proliferation, endpoint for blastocyst quality and growth (Shin et al., 2018).

In summary, 24 h and anti-γH2AX were the most common exposure time and antibody used. The induction of oxidative stress and apoptosis were the main toxicological effects related to AFB1-contamination.

3.1.1.2. In vivo toxicity. In vivo AFB1-IF studies were performed exposing rats and mice between 8 and 10 weeks to concentrations ranging 0.016–0.07 mg AFB1/kg administered intraperitoneally and orally. No natural compounds against AFB1-toxicity have been tested.

3.1.1.2.1. Neurotoxicity. As shown in Table 2, the only neurotoxicity study was sub chronic (8 weeks) and performed through a microscopic analysis, assessing the effect of AFB1 on different brain sections. The fluorescent quantification of neuronal and astrocyte biomarker, NeuN and GFAP proteins, demonstrated that a low concentration of AFB1 decreased the vitality of neuronal cells in rat hippocampus. Moreover, AFB1 altered the distribution of astrocytes in brain, causing astrogliosis with inflammation and neuronal cell death. Nevertheless, AFB1-withdrawal reversed changes in cerebral cortex and hippocampus (Bahey et al., 2015).

3.1.1.2.2. Immunotoxicity. In the longest exposure (8–10 weeks), AFB1 promoted the diffusion of Epstein–Barr virus (EBV), which markedly increased the incidence of Burkitt lymphoma. In addition, AFB1 induced EBV-driven cellular transformation in humanized animal model. Owing to the activation of EBV lytic cycle, the expression of EB-nuclear antigen and EBV replicative load was significantly increased. In view of this, AFB1 can be considered a co-factor of EBV mediated-carcinogenesis and immunotoxicity (Accardi et al., 2015).

To sum up, a similar exposure time (8 weeks) in both analyzed studies was observed.

3.1.2. Flow cytometry

3.1.2.1. In vitro toxicity. *In vitro* AFB1-FCM studies exposed cells between 2 h and 72 h to doses of 3.12×10^{-3}-100 μg/ml (Table 3). As shown in Fig. 5, HepG2 was the most used cell line. The protective role of different compounds (GZn, $ZnSO_4$, Zn-Bent1, PKC, acid gallic, IgY, L-Proline) was also investigated.

3.1.2.1.1. Immunotoxicity. As reported above, AFB1 induced a complete autophagic process in macrophages with ETs generation in a dose-dependent manner (Table 3). FCM analysis revealed AFB1-capacity to exacerbate immunotoxicity by switching macrophages polarization to pro-inflammatory M1 phenotype (An et al., 2017).

Mehrzad et al. (2018) evaluated the effect of AFB1 in MDCCs cells. AFB1 impaired the phagocytosis capacity of MDDCs, promoted cell death and dysregulated the function of key cytokines. Similar results were obtained by the same authors by treating human, canine and bovine leukocytes with low doses of AFB1. As expected, an aberrant activation of caspase 3/7 and a significant decrease of ATP content was observed. FCM-analysis showed a slightly increase of necrotic neutrophils, lymphocytes, and monocytes in all studied models (Mehrzad et al., 2020).

In human lymphocytes, the induction of oxidative stress, lipid peroxidation, with the suppression of superoxide dismutase (SOD) activity were obtained upon AFB1-exposure. Interestingly, FCM was used to detect the 8-oxyguanine (8-oxoG), a typical marker of DNA/RNA oxidative damage. The presence of 8-oxoG may promote mismatches during DNA replication and miscoding in transcriptomic process, thus inducing genetic mutations. The content of 8-oxoG in samples increased in an AFB1-dose-dependent manner (Su et al., 2017).

Sun et al. (2018) confirmed that exposure to toxin promoted the switch of macrophages and SIV-infection, as demonstrated by the increase of viral titers and NP expression. Moreover, the promotion of inflammation and cell death in a concentration-dependent manner was observed.

In the same cell line, exposure to the same AFB1-doses elicited cell death in a dose-dependent manner via mitochondrial pathway. In comparison to the control, nuclei changes with chromatin condensation, marginalization and fragmentation were observed in AFB1-treated cells. Another important immune index for macrophages is the phagocytic activity, which was significantly decreased. The promotion of oxidative stress with ROS generation and a decreased glutathione (GSH) activity was also detected (Zhou et al., 2019). Similar results were obtained by Hou et al. (2018) who showed that the combined action of AFB1 and OTA exacerbated immunotoxicity due to the marginalization, condensation and fragmentation of chromatin with apoptotic bodies formation. Moreover, the expression of pro-inflammatory cytokines (TNF-α and IL-6) significantly increased while the release of lactate dehydrogenase and phagocytic index decreased. Mycotoxin-exposure also stimulated the production of free radicals with a significant decrease of GSH activity.

3.1.2.1.2. Hepatotoxicity. After a short exposure, AFB1 sparked mitochondrial-ROS generation, decreased MMP and induced apoptosis via Nrf2-signal pathway activation. Moreover, the altered expression of caspase 3/9, NADPH quinine oxidoreductase 1, SOD and HO-1 has been observed (Liu and Wang, 2016). Similarly, 24 h exposure to toxin caused apoptotic bodies formation and arrested the cell cycle at phase S with marked genomic alterations. AFB1 inhibited the global DNA hypomethylation and induced intracellular ROS generation with mitochondrial dysfunctions (Yang et al., 2016). Interestingly, AFB1-exposure could enhance the migration of hepatocellular carcinoma cells to other tissues. A decreased cell ratio at G_0/G_1 phase and an increased cell distribution at G_2/M stage confirmed the aberrant growth and the subsequent extra-tissue expansion of cancer cells (K. Chen et al., 2016).

Furthermore, AFB1 alone or in combination with Fumonisin B1 (FB1) increased both the production of ROS and the percentage of apoptotic cells (10–30% more in comparison to the control) with a significant decrease of MMP in a dose-dependent manner. A significant increase of oxidative stress might contribute to cell apoptosis by disrupting the mitochondria, leading to the release of cytochrome *c* (cyt *c*), and activating caspase cascade. Additionally, the cell cycle arrest at phase S was associated with the reduced DNA content in AFB1-treated cells (Du et al., 2017).

Oskoueian et al. (2015) demonstrated that PKC and acid gallic played an important cytoprotective effect on chicken hepatocytes by inhibiting the lipid peroxidation and cell death induced by AFB1. Phenolics compounds (PEF) improved the antioxidant cell system, through the production of SOD, catalase (CAT) and glutathione reductase (GR). As an excessive amount of ROS promoted the NF-kB up-regulation and NRF2 down-regulation and induced the expression of several pro-inflammatory mediators (IL-6, TNF-α), PEF may attenuate cell inflammation due to the direct inhibition of oxidative stress.

In HepG2 cells, the identification and quantification by FCM analysis of three different and typical markers of cancer stem cells, CD133, CD44, and aldehyde dehydrogenase1 upon AFB1-exposure demonstrated its capacity to promote hepato-cellular carcinoma development (Ju et al., 2016).

A similar duration study revealed that high concentrations of AFB1 triggered apoptotic bodies formation and DNA damage with cell cycle arrest at G_2/M phase. The aberrant ROS production (1.5-fold higher than control) with MMP disturbance has been also observed. Nevertheless, low doses of IgY showed protective effects against oxidative stress, apoptosis and cell cycle arrest associated with AFB1-treatment (Qiu et al., 2018).

3.1.2.1.3. Gastrointestinal toxicity. In relation to gastrointestinal toxicity, the molecular explanation on the risks of cross-talk between AFB1 and OTA was provided in intestinal cancer cells by Kim et al. (2016). DNA fluorescence analysis performed by fluorescence-activated cell sorting (FACS) technique revealed that AFB1 was capable to trigger genomic damages, apoptosis and cell cycle arrest at phase S via p53 dysregulation. These mutagenic effects were strongly antagonized by OTA-treatment which may contribute to cancer cells survival by increasing the risk of carcinogenesis.

Nones et al. (2017) demonstrated the cytoprotective effect of Zn-Bent1 against fungal compounds. Low doses of Zn-Bent1 reversed the elevated percentage of apoptotic nuclei and necrotic cells promoted by AFB1 (15% more than control). Likewise, in Caco-2, AFB1 triggered a steady state level of permeabilized PI positive cells indicating necrosis/late apoptosis, whereas in HCT116 cells, AFB1 caused apoptosis in a dose-dependent manner with a significant arrest of cell cycle at G_2/M phase (Gauthier et al., 2020).

3.1.2.1.4. Nephrotoxicity. One of the main organs affected by AFB1-toxicity is undoubtedly the kidney. Regarding the most severe exposure reported, AFB1 (100 μg/ml) activated oxidative stress-related pathways and caused kidney injury with a high rate of apoptotic cells (70% more in comparison to the control). However, L-proline preserved kidney integrity alleviating oxidative damage and decreasing downstream apoptosis by regulating proline dehydrogenase levels and pro-apoptotic proteins expression (Li et al., 2019). Furthermore, acute exposure to AFB1 has promoted the alteration of p21 and its specific regulators, PLK1, PLD1 and MYC, thus causing a significant arrest of cell cycle at phase S in a dose-dependent manner. Since p21 is the most important regulator of G_1/S and S/G_2 cell cycle transition, DNA replication and genomic stability, the alteration of cell cycle has been considered as the main cytotoxic effect of AFB1 in kidney cells (Huang et al., 2019).

3.1.2.1.5. Neurotoxicity. Although different studies have suggested AFB1-ability to cross the BBB and disrupt its integrity, the effects on brain are not well reported. In mouse astrocytes, AFB1 led to an aberrant cell death (16.55% higher than control) in a time-dependent manner with ATP depletion and caspases 3/7 activation. Significant cyt *c* release confirmed the association between apoptosis and mitochondrial impairment (Vahidi-Ferdowsi et al., 2018). In a similar way, AFB1 may provoke microglial cell death due to the intracellular ATP depletion and

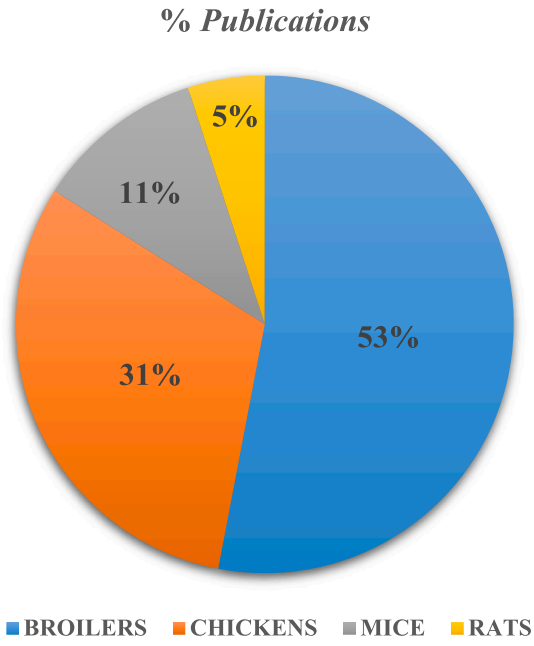

Fig. 6. Percentage of publications (n = 18) according to animal models used in AFB1-FCM *in vivo* studies.

caspase 3/7 activation. Additionally, toxin could trigger an inflammatory reaction in neuronal cells by the dysregulation of many pro-inflammatory cytokines such as TRLs, NF-κB and myeloid differentiation primary response 88 (MyD88). In view of this, AFB1 could increase the susceptibility to neurodegenerative diseases, inducing neuroinflammation and altering the homeostasis of human CNS (Mehrzad et al., 2018a,b).

3.1.2.1.6. Breast toxicity. Finally, the harmful effects of AFB1 have also been studied in BME cells. Wu et al. (2021) observed the cell cycle arrest, inhibition of cell proliferation and apoptosis upon AFB1-exposure. The cytotoxicity was related to epigenetic modifications; in particular, a marked decrease of RNA methylation was detected.

In summary, 24 h and 48 h were the most common exposure times in FCM assay while the apoptosis assay was the main analysis performed. The enhancement of apoptosis and cell cycle arrest were the main toxicological effects observed owing to AFB1-treatment.

3.1.2.2. In vivo toxicity. In vivo AFB1 FCM-studies, the exposure time ranged between 1 and 6 weeks with concentrations of 0.016–1.25 mg/kg administered orally, by gavage or in contaminated feed in broilers, chickens, mice and rats (Fig. 6). The activity of non-pathogenic bacteria (LAB, LP) and natural compounds (MT, Se, β-1,3-glucan) was investigated.

3.1.2.2.1. Immunotoxicity. In a sub-acute immunotoxicity study, AFB1 markedly decreased the percentages of lymphocytes subsets, Foxp3+ T cells, and reduced IL-2, TNF-α, IL-17 and IFN-γ production. Also, it has been demonstrated that AFB1 led to a general immune suppression by the down-regulation of Th1,Th2,Th17 and Treg genes related to immune responses. However, β-1,3-Glucan improved the responses of lymphocyte subsets, including cytokines production, thus counteracting AFB1-immunotoxicity in spleen (Bakheet et al., 2016). Similarly, AFB1, alone or in combination with FB1, promoted DNA-damage and oxidative stress by increasing caspase-3 activity and IL-4, IL-10 expression. The activity of antioxidant enzymes (Gpx and SOD) was clearly reduced. However, LAB-administration induced protective effects against oxidative stress and immunotoxicity of both mycotoxins (Abbès et al., 2016). Likewise, the pre-treatment with LP BEJ01 and MT prevented the effects of AFB1 on immune response in rats. The protective effects of these compounds could be explained by their ability to bind the toxin in the gastrointestinal tract, thereby reducing its bioavailability. Otherwise, exposure to AFB1 caused inflammation and oxidative stress with a marked reduction of immunoglobulins, B and T-lymphocytes, and natural killer cells (Ben Salah-Abbes et al., 2016).

Noteworthy in Table 4, the presence of several studies with similar experimental conditions, in which AFB1-toxicity and the possible protective role of selenium on chickens and broilers immune organs were investigated. Histopathology and FCM analysis demonstrated the negative effect of AFB1-dietary exposure (0.6 mg/kg) in chickens bursa of Fabricius (BF). AFB1 arrested the cell cycle in G_2/M phase at 7 days and in phase G_0/G_1 at 14 and 21 days. The arrest of cell cycle was related to alterations in Cyclin D1 signaling pathway (Hou et al., 2018a). These toxicological damages were restored by the dietary supplementation of Se (0.4 mg/kg), which also alleviated histological lesions and oxidative damage induced by AFB1-administration (Hu et al., 2018b). Chickens treated with AFB1 for 21 days have shown a clear splenocytes death (10–15% higher than control group) due to the impairment of death receptors (FAS, FASL, TNF-α, TNF-R1) and ER molecules expression (Grp78 and Grp94) (Zhu et al., 2017). Fang et al. (2019) demonstrated that these molecular alterations could be reversed by Se-supplementation (0.4 mg/kg) in contaminated feed.

In broilers thymocytes, Se could alleviate AFB1-induced cell death and histological lesions and may reversed the G_0/G_1 cell cycle arrest by modulating p21/p27-CyclinE/Cdk2 and p15-CyclinD1/Cdk6 signaling pathways (Guan et al., 2019). In a similar duration exposure (3 weeks), AFB1 (0.15, 0.3, 0.6 mg/kg) induced apoptosis by altering caspase-3, Bax, Bcl-2 expression in broilers thymus and BF (Peng et al., 2016).

Furthermore, consumption of AFB1-contamined feed was associated with immunosuppression in broilers spleen. In particular, ROS-induced apoptosis, DNA damage and mitochondrial impairment have been observed (J. Chen et al., 2016). In a 21 days study, AFB1 compromised the rate of cell-mediated immunity in broilers cecal tonsil. Authors obtained a clear reduction in cytokines (IL-2, IL-4, IL-6, IL-10, IL-17, IFN-γ, TNF-α) expression and a reduced percentage of T-cells subset ($CD3^+$, $CD3^+CD4^+$,$CD3^+CD8^+$) (Liu et al., 2016). Whilst, in broilers spleen, thymus and BF the ingestion of AFB1-contaminated feed during 42 days caused histopathological lesions with lymphocytes depletion. In this case, AFB1-MOA was associated with alterations in mitochondrial and ER compartments (Peng et al., 2015).

Finally, the different sensitivity of broilers BF and thymus to mycotoxin-exposure in contaminated feed during 42 days was evaluated. Histopathological lesions and pathological impairment were evident to a greater extent in BF than thymus with higher lymphocyte depletion. At 21 days, both thymocytes and BF cells showed a cell cycle arrest at phase G_2/M. Whilst, at 42 days, cell cycle perturbations at phase G_0/G_1 in thymocytes and at G_2/M phase in BF cells was observed. However, a similar apoptotic rate was obtained (Peng et al., 2017).

3.1.2.2.2. Hepatotoxicity. Table 4 shows that the ingestion of AFB1-contamined feed (0.6 mg/ml) during 21 days caused degenerative histological lesions in broilers liver with high percentages of apoptotic cells (2-5-fold higher than control group) and intracellular ROS production. Se-treatment (0.4 mg/ml) could mitigate oxidative stress and relieve AFB1-induced apoptosis through the molecular regulation of death receptors (Wu et al., 2019).

3.1.2.2.3. Gastrointestinal toxicity. To evaluate the effects of AFB1 on the gastrointestinal tract, chickens and broilers were exposed to a sub-acute contamination. It has been observed marked morphological changes in chickens jejunum with a reduction of villus height and area. In this case, the apoptosis of jejunal cells was associated with the altered expression of death receptors and ER molecules (Zheng et al., 2017). Fang et al. (2018) observed the protective role of Se against AFB1-toxicological damages by modulating the ataxia telangiectasia mutated (ATM) pathway and by reversing G_2/M cell cycle arrest.

In broilers jejunal cells, Yin et al. (2016) demonstrated that ATM kinase and its downstream molecules, the checkpoint kinase Chk2 and

Table 4
AFB1-FCM studies: *In vivo* model, dose and exposure time, FCM assay, mechanism and references.

In vivo model	Dose administration	Exposure time	FCM assay	Mechanism	References
Immunotoxicity					
Mice spleen	1.25 mg/kg + β-1,3-Glucan (150 mg/kg)/ orally	1 week	Measurement of IL-2, TNF-α, IL-17, IFN-γ Assessment of intracellular Foxp3 Assessment of cell surface markers	Reduction of T-cells subset and cytokines production.	Bakheet et al. (2016)
Mice thymus	0.08 mg/kg + LAB (2 mg/kg)/orally	2 weeks	Apoptotic DNA analysis	Increase of intracellular ROS production, high level of apoptotic DNA and cell death.	(Abbès et al., 2016)
Rats plasma	0.08 mg/kg + *Lactobacillus paracasei* BEJ01 (2 mg/kg) + montmorillonite clay (0.5 mg/kg)/gavage administration	2 weeks	Measurement of total white and red blood cells and lymphocyte subtypes	Enhancement of oxidative stress with a reduction of B-lymphocytes, T-lymphocytes, NK cells subset.	Ben-Salah Abbes et al. (2016)
Chickens bursa of Fabricius	0.6 mg/kg/contaminated diet	3 weeks	Cell cycle analysis	Cell cycle arrest.	(Hou et al., 2018a)
Chickens bursa of Fabricius	0.6 mg/kg + Se (0.4 mg/kg)/ contaminated diet	3 weeks	Cell cycle analysis	Tissue damage and cell cycle arrest.	Hu et al. (2018b)
Chickens spleen	0.6 mg/kg/contaminated diet	3 weeks	Apoptosis assay	Induction of apoptosis with the expression of death receptor and endoplasmic reticulum molecules.	Zhu et al. (2017)
Chickens spleen	0.6 mg/kg + Se (0.4 mg/kg)/ contaminated diet	3 weeks	Apoptosis assay	Aberrant apoptotic rate.	Fang et al. (2019)
Broilers thymus	0.6 mg/kg + Se (0.4 mg/kg)/ contaminated diet	3 weeks	Cell cycle analysis	Alterations in cell cycle.	(Guan et al., 2019)
Broilers thymus and bursa of Fabricius	0.15, 0.30, 0.60 mg/kg/contaminated diet	3 weeks	Apoptosis assay	Promotion of apoptosis.	Peng et al. (2016)
Broilers spleen	0.15, 0.30, 0.60 mg/kg/contaminated diet	3 weeks	Apoptosis assay	Induction of oxidative stress, splenocytes apoptosis and immunodepression.	(J.Chen et al., 2016)
Broilers cecal tonsil	0.6 mg/kg/contaminated diet	3 weeks	T cells identification	Reduction of T cell subsets and cytokines production.	Liu et al. (2016)
Broilers immune organs	0.082, 0.134 mg/kg/contaminated diet	6 weeks	Apoptosis assay	Promotion of apoptosis, histopathological lesions with lymphocytic and splenic plasmacytes depletion.	Peng et al. (2015)
Broilers thymus and bursa of Fabricius	0.016, 0.134 mg/kg/contaminated diet	6 weeks	Cell cycle analysis Apoptosis assay	Cell cycle arrest and pathological impairment.	Peng et al. (2017)
Hepatotoxicity					
Broilers liver	0.6 mg/kg + Se (0.4 mg/kg)/ contaminated diet	3 weeks	Apoptosis assay	Induction of apoptosis and ROS generation.	Wu et al. (2019)
Gastrointestinal toxicity					
Chickens jejunum	0.6 mg/kg/contaminated diet	3 weeks	Apoptosis assay	Induction of apoptosis with the altered expression of death receptor and endoplasmic reticulum molecules.	Zheng et al. (2017)
Chickens jejunum	0.6 mg/kg + Se (0.4 mg/kg)/ contaminated diet	3 weeks	Cell cycle analysis	Pathological impairments and cell cycle alteration.	Fang et al. (2018)
Broilers jejunum	0.6 mg/kg/contaminated diet	3 weeks	Cell cycle analysis	Cell cycle arrest.	Yin et al. (2016)
Nephrotoxicity					
Broilers kidney	0.3 mg/kg + Se (0.4 mg/kg)/ contaminated diet	3 weeks	Apoptosis assay Cell cycle analysis	Reduction of cell proliferation and arrest of cell cycle in G_0/G_1 phase.	Yu et al. (2015)

the increased expression of p53 and p21, likely contribute to the AFB1-induced G_2/M cell cycle arrest.

3.1.2.2.4. Nephrotoxicity. In the only study found on nephrotoxicity, Yu et al. (2015) demonstrated that the ingestion of AFB1 (0.3 mg/kg) in contaminated feed during 21 days resulted in apoptosis with altered caspase-3 and Bax expression. A significant reduction of cell proliferation with cell cycle arrest at phase G_0/G_1 was also revealed. However, Se supplied in diet mitigated apoptosis, cell proliferation and kidney damages.

In summary, 3 weeks was the most used exposure time while the apoptosis assay was the main analysis performed. The most used concentrations were 0.6 mg/kg for AFB1 and 0.4 mg/kg for Se in contaminated feed. The induction of apoptosis, cell cycle arrest and immunosuppression were the main damages related to AFB1-administration.

3.2. Ochratoxin A

The toxicity of OTA, the other mycotoxin analyzed in this review, was also investigated using the techniques mentioned above. In relation to IF analysis, antibodies used varied according to the specific pathway studied by authors while the FCM was mainly performed to detect apoptosis, ROS generation, alterations in cell cycle, mitochondrial and redox balance. Furthermore, several natural compounds have been used to mitigate OTA-toxicity, such as luteolin (LUT), selenomethionine (SeMet), taurine (TAU), melatonin, NAC, resveratrol (RSV), zinc, N-acetyl-tryptophan (NAT), glycyrrhizin (CAG), gluconolactone (GA), L-arginine (L-Arg), silymarin (Sil) and astragalus polysaccharide (APS).

For each technique, the selected OTA-studies were organized according to the model used showing that the main toxicological effects *in vitro* are nephrotoxicity, gastrointestinal toxicity, hepatotoxicity, immunotoxicity, embryotoxicity, reproductive toxicity, neurotoxicity,

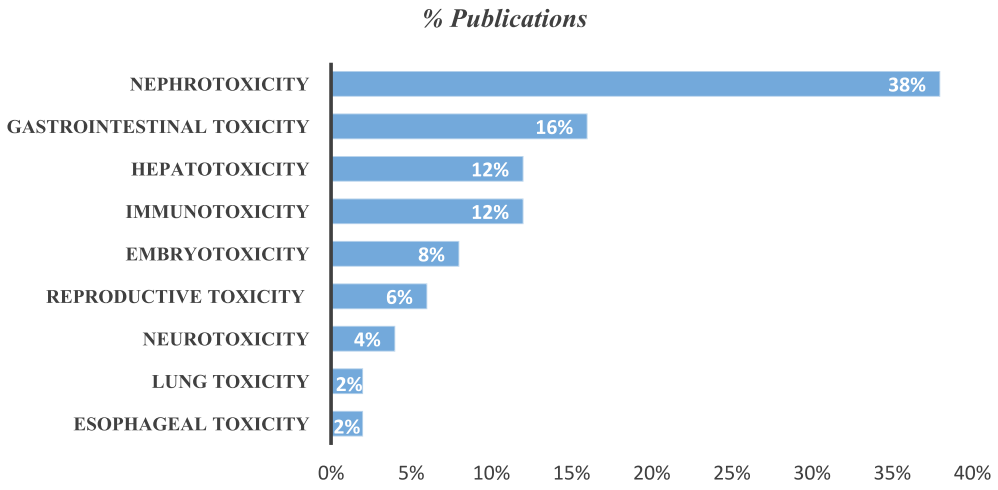

Fig. 7. Percentage of publications (n = 50) according to the main toxicological effects of OTA *in vitro*.

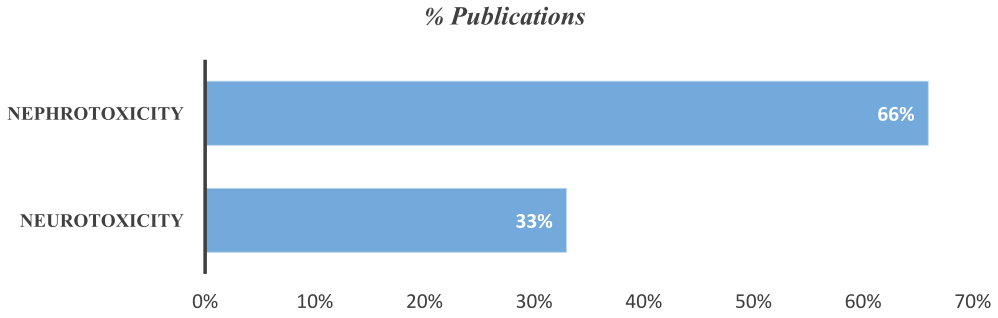

Fig. 8. Percentage of publications (n = 3) according to the main toxicological effects of OTA *in vivo*.

lung and esophageal toxicity (Fig. 7). Whilst, only three *in vivo* toxicity studies have been selected, which confirmed OTA-nephrotoxicity and neurotoxicity (Fig. 8). The summary of the articles found for OTA are shown below. Tables were divided depending on the technique, model used and type of toxicity, and were ordered by the exposure time, from the shortest to the longest.

3.2.1. *Immunofluorescence*

3.2.1.1. In vitro toxicity. Exposure times chosen for *in vitro* OTA-IF studies ranged between 2 h and 40 weeks with concentrations of 1 × 10^{-2}- 40 μg/ml (Table 5). Fig. 9 shows that PK-15 was the most used cell line. LUT, SeMet, NAC, TAU and melatonin were employed to alleviate OTA-toxicity.

3.2.1.1.1. Immunotoxicity. In the only study reported, OTA impaired the phagocytosis function of heterophils and enhanced the release of their ETs. The IF analysis of ETs main constituents, histone H3 and elastase, proved their dose-dependent release. In addition, ETs formation was associated with the activation of NADPH oxidase, ERK1/2, and p38/MAPK signaling pathways, which led to intracellular ROS generation (Han et al., 2019).

3.2.1.1.2. Hepatotoxicity. As shown in Table 5, the only study reviewed was conducted by Shen et al. (2020). It has been proved that OTA-dichlorination (OTA Cl/M) and demethylation (OTA M) triggered the downregulation of pregnane X receptor (PXR), whose excessive activation is related to lipid retention, metabolic diseases and toxicological bioactivation of drugs. The fluorescence staining of FLAG, which is widely used as an epitope tag for selective protein detection, showed that OTA and its derivatives interacted with different residues of PXR, providing the molecular basis for a selectivity. In view of this, OTA-derivatives (C1/M and M) may be considered novel PXR-antagonists, reducing liver cytotoxicity.

3.2.1.1.3. Gastrointestinal toxicity. The gastrointestinal tract is one of the main sites affected by OTA-toxicity (Ricci et al., 2021). After a short exposure, this mycotoxin not only promoted cytotoxicity but also the phosphorylation and nuclear translocation of ERK1/2, which in turn mediated the autophagy, reduced mitochondrial ROS production and caspase-3 activation and mitigated OTA-detrimental effects. Therefore, OTA may have a bivalent effect on IPEC-J2 cells whereas ERK1/2-mediated autophagy could be considered as one of the main protective mechanisms in maintaining the integrity of intestinal barrier (Wang et al., 2018).

In GES-1 cells, Li et al. (2019) demonstrated that an over-activation of autophagy may produce opposite results. Indeed, OTA-exposure promoted the conversion of LC3B-I to LC3B-II, a typical autophagy marker, indicating that autophagic-cell death was triggered. Moreover, it has been detected an excessive production of autophagic vacuoles, which engulfed the damaged mitochondria and induced the occurrence of mitophagy. In this case, mitophagy was positively related to cell death. Authors concluded that OTA-effects on mitochondria in GES-1 cells are complex as it not only promoted apoptosis via mitochondrial pathway but also enhanced mitochondria biogenesis via AMPK/PGC-1α/TFAM pathway, increasing cell survival.

In similar duration exposure, OTA alone or in combination with DON, compromised the intestinal barrier integrity, with a decreased transepithelial electrical resistance (TEER) value (50% less than control cells) and an increased paracellular permeability (2-fold higher in comparison to the control). In addition, the fluorescent analysis of claudin-3 and 4 tight junction and p65 factor demonstrated that OTA was capable to exacerbate DON-induced intestinal barrier dysfunction, inflammation and pro-inflammatory cytokines production (Ying et al., 2019). Interestingly, the analysis conducted by Nakayama et al. (2018)

Table 5
OTA-IF studies: *In vitro* and *in vivo* model, dose and exposure time, antibodies implemented, mechanism and references.

In vitro/in vivo model	Dose administration	Exposure time	Antibodies used	Mechanism	References
In vitro Immunotoxicity					
Chicken heterophils	2,4,8 μg/ml	2 h	Anti-NE, anti-histone H3	Disruption of ETs formation and intracellular ROS generation.	Han et al. (2019)
Hepatotoxicity					
hPXR-HRE cells	0.40 μg/ml	24 h	Anti-FLAG	Cytotoxicity.	Shen et al. (2020)
Gastrointestinal toxicity					
IPEC-J2 cells	0.80 μg/ml	12 h	Anti-ERK1/2	Induction of autophagy, apoptosis and ROS generation. Disruption of intestinal barrier.	Wang et al. (2018)
GES-1 cells	4 μg/ml	24 h	Anti- LC3B, anti α-tubulin	Mitochondrial dysfunction with autophagy, cell death and oxidative stress promotion.	Li et al. (2019)
IPEC-J2	1.6 μg/ml	24 h	Anti-p65, anti-claudin-3, anti-claudin-4	Intestinal barrier dysfunction and inflammatory response.	Ying et al. (2019)
CMT93-II cells	16 μg/ml	36 h	Anti-claudin-2, anti-claudin-4, anti-claudin-6	Disruption of intestinal barrier.	Nakayama et al. (2018)
Caco-2 cells	8×10^{-2}, 8 μg/ml	48 h	Anti-claudin-3, anti-claudin-4, anti-occludin, anti-ZO1	Disruption of epithelial barrier permeability.	(Gao et al., 2018)
GES-1 cells	1 μg/ml	72 h for (40 weeks)	Anti-β-catenin	Promotion of cell malignant transformations via intracellular ROS generation.	Jia et al. (2016)
Nephrotoxicity					
NRK-52E cells	20 μg/ml + LUT (28.6 μg/ml)	24 h	Anti-Nrf2, anti-HIF- 1α	Promotion of oxidative stress, lipid peroxidation and mitochondrial dysfunction.	Liu et al. (2020)
HKC cells	2,4,8,16 μg/ml	24 h	Anti-DNMT1	Cell cycle alteration and epigenetic modifications.	Zhang et al. (2020)
HKC cells	4 μg/ml	24 h	Anti-Grp75, Anti-α SMA, anti 8-hydroxyguanosine	DNA damage, oxidative stress and disruption of mitochondrial metabolism.	Yang et al. (2019)
MDCK cells	0.5, 1.0, 2.0 μg/ml	24 h	Anti-NLRP3	Promotion of cell death, inflammation and kidney fibrosis.	Li et al. (2021)
HMC cells	0.80, 1.60, 3.20 μg/ml	48 h	Anti-vimentin, anti-p65	Induction of cell morphologic changes, fibrosis, DNA damage and ROS production.	Le et al. (2020)
PK-15 cells	4×10^{-2} μg/ml + NAC (815 μg/ml)	48 h	Anti-PCV2	Enhancement of autophagy and porcine circovirus type 2 replication.	Qian et al. (2017)
PK-15 cells	0.01, 0.05, 0.1, 0.5,1 μg/ml + NAC (652 μg/ml)	48 h	Anti-PCV2	Promotion of porcine circovirus type 2 replication and oxidative stress.	Gan et al. (2015a)
PK-15 cells	4×10^{-2} μg/ml + SeMet (0.156, 0.312, 0.468 μg/ml)	48 h	Anti-PCV2	Induction of autophagy of porcine circovirus type 2 replication.	Qian et al. (2018)
PK-15 cells	4×10^{-2} μg/ml + TAU (1250, 2500, 5000 μg/ml)	60 h	Anti-PCV2	Promotion of autophagy and porcine circovirus type 2 replication.	Zhai et al. (2018)
Neurotoxicity					
Neural stem cells	1×10^{-2}, 0.1, 1, 10, 100 μg/ml	5 days	Anti-GFAP, anti-DCX	Reduction of cell proliferation and differentiation rates with a significant decrease in neuroblasts and glial cells.	Paradells et al. (2015)
Neural stem cells	2×10^{-2}, 8×10^{-2}, 0.40, 2 μg/ml	7 days	Anti-MAP2 clone M13, Anti-MAP2 clone AP18, Anti- Doublecortin, Anti-GFAP, Anti-Nestin, Anti-A2B5, Anti-mGalc	Impairment of neural differentiation.	Gill & Kumara (2019)
Embryotoxicity					
Mouse oocytes	3 μg/ml	16 h	Anti-Gpx, anti-α-tubulin, anti-H3K9ac, anti-H3K9me3	Induction of oxidative stress, cell apoptosis, epigenetic modifications and meiotic failure.	Jia et al. (2020)
Porcine ovarian granulosa cells	8,16 μg/ml	24 h	Anti-BAX, anti-BCL-2, Anti-ITGB1, anti-F2R	High ROS levels and apoptosis.	Zhang et al. (2019)
Porcine ovarian granulosa cells	8,16 μg/ml	24 h	Anti-ATR, anti-γ-H2AX, anti- Rad51, anti-Brca1	DNA damage and alterations in cell proliferation.	Zhang et al. (2020)
Porcine oocytes	3.20 μg/ml + Melatonin (2.30 $\times 10^{-4}$, 2.30 $\times 10^{-2}$, 2.30, 230 μg/ml)	27–52 h	Anti-α-tubulin, anti-LC3A	Mitochondrial impairment, promotion of oxidative stress, early apoptosis and autophagy.	Lan et al. (2020)
Reproductive toxicity					
TM3-TM4 cells	0.80, 2 μg/ml	24 h	Anti-PCNA		

(*continued on next page*)

Table 5 (*continued*)

In vitro/in vivo model	Dose administration	Exposure time	Antibodies used	Mechanism	References
				Suppression of Sertoli and Leydig cell proliferation. Failure of spermatogenesis.	Park et al. (2020)
Sperm cells	4, 40 μg/ml	24 h	Anti-PTEN, Anti-PI3K, Anti-AKT, Anti-p-AKT	ROS production and cell death with a reduction of sperm motility.	Zhang et al. (2018)
In vivo Nephrotoxicity					
Mice kidney	2.50 mg/kg/intraperitoneally	3 weeks	Anti-vimentin, anti-collagen I, anti-p53, anti-caspase 3, anti-CD45, anti-HO-1	Promotion of inflammation, apoptosis, oxidative stress.	Loboda et al. (2017)
Neurotoxicity					
Mice brain	3.50 mg/kg/intraperitoneally	6 weeks	Anti-GFAP, anti-Iba1, anti-beta III Tubulin, anti-Dcx, anti-calretinin.	Impairment of neurogenesis and brain development.	Paradells et al. (2015)

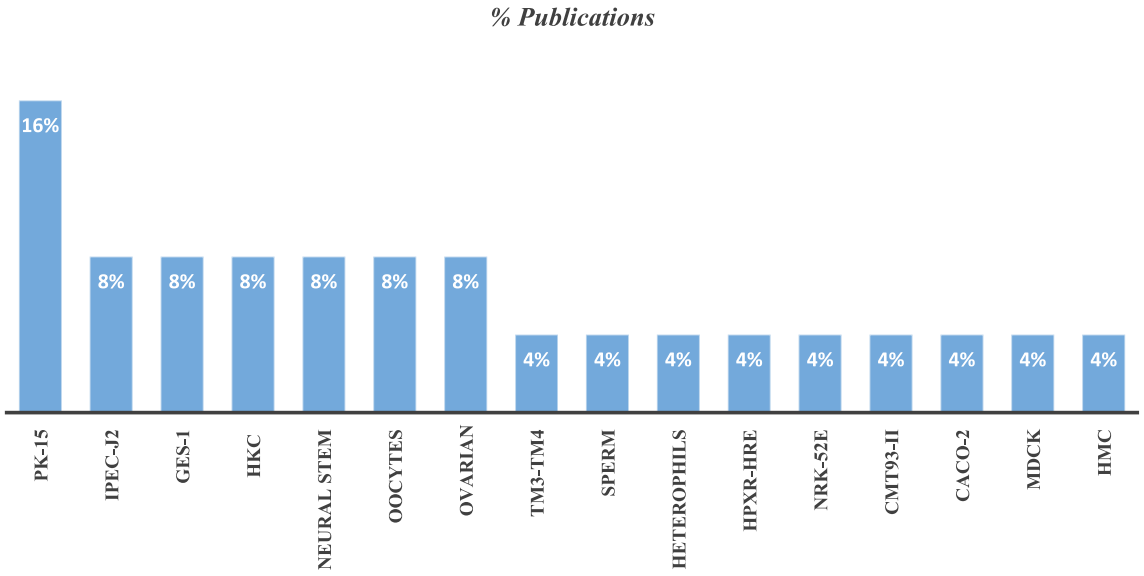

Fig. 9. Percentage of publications (n = 25) according to cell lines used in OTA-IF *in vitro* studies.

on claudin-2, a specific tight junction localized and expressed only in the deep crypt of the intestine. In CMT93-II cells, which exhibit typical features of deep crypt cells, OTA reduced claudin-2 expression and altered the TEER, by disrupting the intestinal barrier integrity. A reduced expression of claudin 4 and 6 has been detected as well. Similarly, in differentiated Caco-2 cells, the epithelial integrity was disordered due to an increased paracellular permeability and a decreased TEER value. Microscopic analysis, performed on claudin 3 and 4, occludin and ZO-1, revealed their altered expression and structure. A partial involvement of p44/42 mitogen-activated protein kinase (MAPK) in OTA-mediated intestinal barrier disruption has been observed (Gao et al., 2018).

Finally, chronic exposure to OTA (3 days of mycotoxin-exposure each week during 40 weeks) increased the proliferation, migration, and invasion capacity of GES-1 cells. Authors demonstrated that malignant transformations of GES-1 cells can be attributed to Wnt/β-catenin signaling pathway. Indeed, aberrant de-regulation of Wnt/β-catenin pathway has been closely related to various types of tumors, including gastric cancer. In addition, inoculation of OTA-treated GES-1 cells in mice triggered the formation of tumor xenografts, confirming OTA-carcinogenicity *in vivo*. The pre-treatment with a high concentration of NAC could mitigate the long-term OTA-toxicity via Wnt/β-catenin pathway inhibition (Jia et al., 2016).

3.2.1.1.4. Nephrotoxicity. According to the main target organ related to OTA-toxicity, which is the kidney, the majority of the reviewed studies were focused on nephrotoxicity (Table 5). In NRK-52 E cells, the cytoprotective role of LUT was demonstrated. This compound alleviated OTA-induced oxidative stress by reducing ROS generation and improving the efficiency of antioxidant enzymes (SOD and GSH). Microscopic analysis showed that LUT increased cell antioxidant defenses by activating Nrf2 signaling pathway. At the same time, by modulating HIF-1α pathway, LUT mediated repair and regeneration process, and promoted angiogenesis and endothelial survival (Liu et al., 2020).

In HKC cells, 24 h exposure to toxin suppressed Notch and Ras/MAPK/CREB pathways and impaired cell growth and proliferation. Fluorescence analysis of DNMT1 showed alterations in global DNA methylation, thus correlating OTA-nephrotoxicity with epigenetic changes. The genome-wide hypermethylation may contribute to OTA-mediated the inhibition of cell cycle progression (Zhang et al., 2020).

Interestingly, the analysis carried out by Yang et al. (2019) on 75 kD glucose-regulated protein (Grp75) and mitochondrial factors, involved in cell protection against OTA-activity. Grp75 is a Heat Shock Protein, which regulates the transfer of calcium from ER stores into the mitochondrial matrix. The IF analysis showed a slightly reduction of Grp75 expression and activity, probably related to OTA-contamination, which mediated the inhibition of mitochondrial metabolism. Exposure to toxin was also linked to Lonp1 suppression, a typical marker involved in reducing oxidative stress and in maintaining mitochondrial DNA stability. Fluorescence quantification of 8-OHdG and Kim-1 showed the

tendency of OTA to promote DNA oxidative damage and kidney injury in the examined *in vitro* model.

In the 24 h study, OTA may induce kidney fibrosis by altering α-SMA, vimentin and TNF-β expression in a concentration-dependent manner. At the same time, this mycotoxin enhanced the activation of NLRP3 inflammasome, as detected by the fluorescent quantification of caspase 1-dependent pyroptosis. Also, OTA may promote an inflammatory status by modulating the expression of pro-inflammatory mediators (IL-6, TNF-α) and pyroptosis-related genes (GSDMD, IL-1β, IL-18). These harmful effects were significantly abrogated by MCC950 pre-treatment, a specific NLRP3 inhibitor, and by caspase-1 knockdown (Li et al., 2021).

In a similar study, the fluorescent quantification of vimentin revealed that OTA-administration caused morphological cell changes via ERK1/2 pathway activation. In addition, fluorescence staining of p65 showed its translocation into the nucleus upon IκB-α degradation with the subsequent activation of NF-kB signaling pathway. The pre-treatment with FR180240 and BAY 11–7082, specific inhibitors of ERK1/2 and NF-kB pathways, could withdraw OTA-nephrotoxicity (Le et al., 2020).

As shown in Table 5, several studies with similar experimental conditions, in which OTA-induced autophagy, apoptosis and porcine circovirus 2 (PCV2) replication, were reported. The possible protective role of Se, NAC and taurine was also examined. Qian et al. (2017) observed the increased expression of cap protein and the aberrant viral DNA synthesis upon OTA-administration. However, OTA-induced PCV2-replication was antagonized by NAC-administration. Similar results were obtained by Gan et al. (2015a). In this study, the promotion of PCV-2 replication was associated with p38/ERK1/2 MAPK signaling pathway activation. The cytoprotective role of NAC was also confirmed. Likewise, the pre-treatment with SeMet attenuated OTA-promoted ROS-dependent autophagy and PCV-2 replication by inhibiting AMPK/mTOR signaling pathway (Qian et al., 2018). The same biochemical pathway was modulated by high concentrations of taurine, which could be considered an effective strategy against autophagy, oxidative stress and PCV2 infection (Zhai et al., 2018).

3.2.1.1.5. Neurotoxicity. As shown in Table 5, only two neurotoxicity studies were reviewed. In rat neural stem cells (rNSC), 5 days-exposure to OTA induced morphologic changes, affected cell viability in a concentration-dependent manner and inhibited cell proliferation and neutrospheres formation. Also, the immunostaining of GFAP and Dcx, astrocytes and neurons markers, showed that low doses of toxin significantly decreased neurons maturation and astrocytes density. These results confirmed OTA-negative effects on neural differentiation (Paradells et al., 2015). *In vitro* differentiation of rat NSC into astrocytes, neurons, and oligodendrocytes was also monitored by Gill and Kumara (2019). Using cell-specific IF staining for undifferentiated rNSC (nestin), neutrospheres (nestin and A2B5), neurons (MAP2 clone M13, MAP2 clone AP18, and Dcx), astrocytes (GFAP), and oligodendrocytes (A2B5 and mGalc), OTA-neurotoxicity was confirmed. Indeed, a non-cytotoxic concentration of OTA (0.08 μg/ml) markedly reduced the differentiation degree of rNSC into mature astrocytes, neurons and oligodendrocytes, thereby affecting the normal brain development.

3.2.1.1.6. Embryotoxicity. After 12 h exposure, OTA worsened oocyte quality by impairing meiotic maturation and by disrupting spindle formation and chromosome alignment. Additionally, OTA elicited intracellular ROS production and reduced Gpx activity. The fluorescent quantification of H3K9ac, H3K9me3 revealed the presence of epigenetic alterations in oocytes genome (Jia et al., 2020).

Similarly, microscopic analysis conducted in granulosa cells (GCs) confirmed OTA-ability to activate surface receptors and to promote oxidative stress by decreasing the expression of ITGB 1, a heterodimeric cell-surface receptor involved in different cell functions, and F2R receptor, a G-protein coupled receptor involved in the regulation of GC response. At the same time, fluorescence analysis of Bax and Bcl-2 indicated the positive correlation between OTA-treatment and cell death (Zhang et al., 2019). In the same *in vitro* model, OTA may exert deleterious effects by inducing DNA damage, disrupting DNA repair-related processes and arresting the cell cycle at phase G_2/M. DNA damage was detected by the over-expression of DSB gene, γ-H2AX, and DNA repair-related genes, BRCA1 and RAD51 (Zhang et al., 2020).

In porcine oocytes, Lan et al. (2020) observed disturbances in oocytes maturation owing to the delay of Cdc2-mediated cell cycle progression. The disruption of meiotic spindle formation was also related to fungal exposure. Moreover, IF analysis showed that OTA triggered aberrant mitochondria dysfunctions in oxidative phosphorylation with the promotion of oxidative stress, apoptosis and autophagy. However, the pre-incubation with elevated concentrations of melatonin

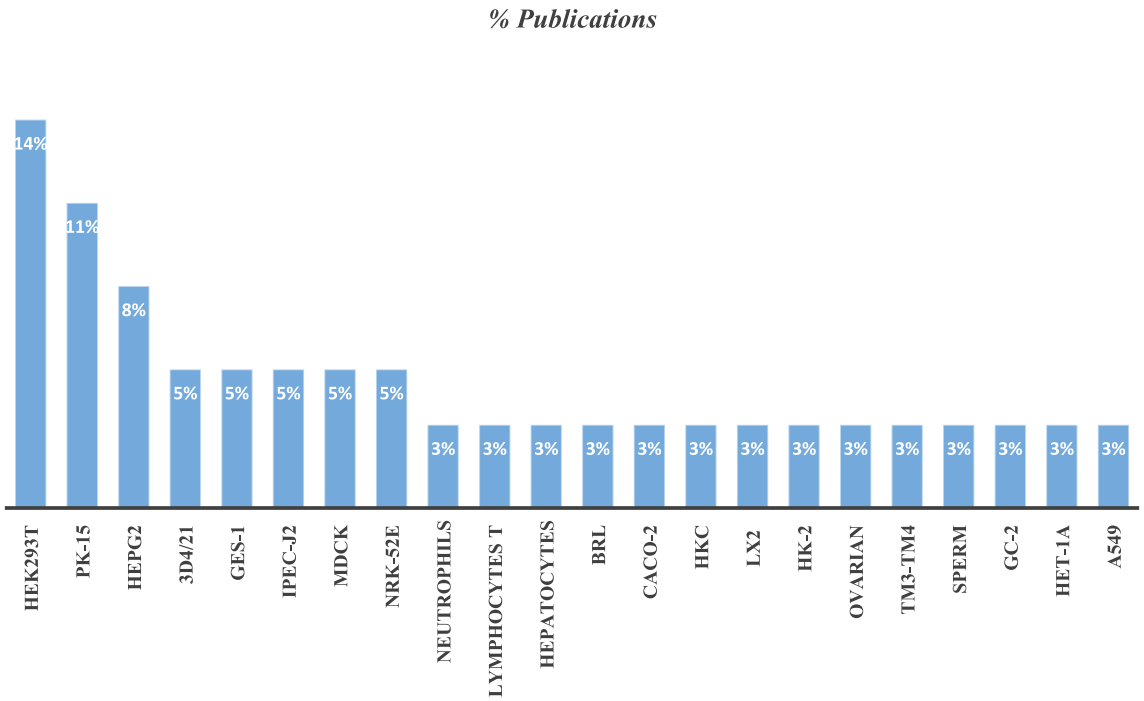

Fig. 10. Percentage of publications (n = 36) according to the cell lines used in OTA-FCM *in vitro* studies.

Table 6
OTA-FCM studies: *In vitro and in vivo* model, dose and exposure time, FCM assay, mechanism and references.

In vitro/In vivo model	Dose administration	Exposure time	FCM assay	Mechanism	References
In vitro Immunotoxicity					
H9 T cells	0.40, 2, 4, 8 μg/ml	3, 6, 12, 18, 24 h	Cell viability Apoptosis assay Detection of caspase-3	Marked changes in cell morphology and DNA fragmentation with high apoptotic rate.	Darif et al. (2016)
Human neutrophils	0–120 μg/ml	4–20 h	Apoptosis assay Mitochondrial membrane potential measurement Intracellular Ca^{2+} measurement	Promotion of neutrophils oxidative burst, apoptosis, ATP depletion and MMP disruption.	Kupski et al. (2016)
3D4/21 cells	1.5 μg/ml + APS (10, 20, 30 μg/ml)	48 h	Apoptosis assays	Induction of pro-inflammatory cytokines expression and cell death.	Liu et al. (2018)
3D4/21 cells	0.1, 0.5, 1, 1.5, 2 μg/ml + NAC (652 μg/ml)	48 h	Apoptosis assay Intracellular ROS measurement	Enhancement of ROS generation, apoptosis and inflammation.	Xu et al. (2017)
Human lymphocytes	1×10^{-3}– 5×10^{-2} μg/ml	72 h	Analysis Th1/Th17 cell differentiation	Promotion of a pro-inflammatory status and RA development.	(Jahreis et al., 2017)
Hepatotoxicity					
HepG2 cells	2, 5, 8, 20 μg/ml	24 h	Apoptosis assays	Promotion of apoptosis, ATP depletion and intracellular structure disruption.	Sali et al. (2016)
Chicken hepatocytes	1 μg/ml + CAG, L-Arg, Sil, GA (1 μg/ml)	24 h	Apoptosis assay	Induction of ROS generation, lipid peroxidation and reduction of antioxidant enzymes activity.	Yu et al. (2018)
HepG2 cells	4,8,12 μg/ml	24 h	Apoptosis assay	Induction of cell death.	Zhu et al. (2016)
BRL cells	6.8, 7.6, 8.4 μg/ml	48 h	Apoptosis assay	Induction of cell death.	Wang et al. (2020)
HepG2 cells	1.25, 2.5, 5, 10 μg/ml	48 h	Cell cycle analysis	Arrest of cell cycle with DNA damage.	(Juan-García et al., 2019)
Gastrointestinal toxicity					
IPEC-J2 cells	0.80 μg/ml	6,12,24 h	Apoptosis assay	Induction of autophagy, apoptosis and ROS generation. Disruption of intestinal barrier.	Wang et al. (2018)
IPECJ-J2 cells	0.80, 1.60, 3.20 μg/ml	12 h	Apoptosis assay	Promotion of apoptosis and ROS generation with impairment in mitochondrial permeability.	Wang et al. (2017)
GES-1 cells	2,4,8 μg/ml	24 h	Apoptosis assay Intracellular ROS measurement Mitochondrial membrane potential measurement Mitochondrial mass determination	Mitochondrial dysfunction with autophagy, cell death and oxidative stress promotion.	Li et al. (2019)
Caco-2 cells	5×10^{-4}, 5×10^{-3}, 4 μg/ml	48 h	Apoptosis assay	Impairment of intestinal function and apoptosis.	Yang et al. (2019)
GES-1 cells	1 μg/mL + NAC (652 μg/ml)	72 h for 40 weeks	Cell cycle analysis Intracellular ROS measurement	Promotion of cell malignant transformation via intracellular ROS generation.	Jia et al. (2016)
Nephrotoxicity					
HEK293T cells	1–10 μg/ml + NAT (2.5 μg/ml)	0.5,1, 4, 24, 48 h	Intracellular ROS measurement Apoptosis assay Cell cycle analysis	Induction of mitochondrial membrane de-stabilization and oxidative stress.	Agarwal et al. (2020)
NRK-52E cells	20 μg/ml + LUT (28.6 μg/ml)	1,3,6,12,24 h	Intracellular ROS measurement	Promotion of oxidative stress, lipid peroxidation and mitochondrial dysfunction.	Liu et al. (2020)
HEK293T cells	8 μg/ml	1, 24 h	Intracellular ROS measurement	Enhancement of ROS generation, cell apoptosis and mitochondrial impairment.	Liang et al. (2015)
HKC cells	4,8,12,16 μg/ml	24 h	Cell cycle analysis	Cell cycle alteration and epigenetic modifications.	Zhang et al. (2020)
LX2 and HEK293T cells	20 μg/ml	24 h	Apoptosis assay	Induction of apoptosis.	Azam et al. (2019)
NRK-52E cells	8, 20 μg/ml	24 h	Intracellular ROS measurement Apoptosis assay	Alteration in OCT1,2,3 expression with oxidative stress and DNA damage.	Qi et al. (2018)
MDCK cells	0.5, 1.0, 2.0 μg/ml	24 h	Determination of Caspase-1	Promotion of cell death, inflammation and kidney fibrosis.	Li et al. (2021)
MDCK cells	1 μg/ml + Zn (6.5 μg/ml)	24 h	Apoptosis assay	ROS generation and apoptosis.	Li et al. (2019)
HEK293T cells	0.60, 3.76 μg/ml + RSV (5.7 μg/ml)	24, 48 h	Intracellular ROS measurement	Promotion of oxidative stress and ROS generation.	Raghubeer et al. (2015)
HEK293T cells	6.4 μg/ml	48 h	Cell cycle analysis	Promotion of cell apoptosis, ROS generation and DNA damage.	Gong et al. (2019)
HK-2 cells	4×10^{-3}, 4×10^{-2} μg/ml.	48 h	Cell cycle analysis	Oxidative stress induction and cell cycle alteration.	Dubourg et al. (2020)
PK-15 cells	0.01, 0.05, 0.1, 0.5 μg/ml + NAC (652 μg/ml)	48 h	Intracellular oxidants assay Intracellular ROS measurement	Promotion of porcine circovirus type 2 replication and oxidative stress.	Gan et al. (2015a)
PK-15 cells		48 h	Intracellular ROS measurement		

(*continued on next page*)

Table 6 (*continued*)

In vitro/In vivo model	Dose administration	Exposure time	FCM assay	Mechanism	References
	4×10^{-2} μg/ml + NAC (815 μg/ml)			Enhancement of autophagy and porcine circovirus type 2 replication.	Qian et al. (2017)
PK-15 cells	0.40, 0.80, 1.60, 2.40 μg/ml + TAU (625 μg/ml)	48 h	Apoptosis assay	Induction of apoptosis.	Liu et al. (2020)
PK15 cells	2.5 μg/ml + SeMet (3.9×10^{-2}, 7.8×10^{-2}, 0.156, 0.312 μg/ml)	48 h	Apoptosis assay Intracellular ROS measurement	Cell death and oxidative stress promotion.	Gan et al. (2015b)
Embryotoxicity					
Porcine ovarian granulosa cells	8,16 μg/ml	24 h	Apoptosis assay	High ROS levels and apoptosis.	Zhang et al. (2019)
Porcine ovarian granulosa cells	8,16 μg/ml	24 h	Cell cycle analysis	DNA damage and alterations in cell proliferation.	Zhang et al. (2020)
Reproductive toxicity					
TM3-TM4 cells	0.20, 0.40, 1 μg/ml	24 h	Cell cycle analysis Intracellular ROS measurement Mitochondrial Ca^{2+} concentration	Suppression of Sertoli and Leydig cell proliferation. Failure of spermatogenesis.	Park et al. (2020)
Sperm cells	4,40 μg/ml	24 h	Apoptosis assay	ROS production and cell death with a reduction of sperm motility.	Zhang et al. (2018)
GC-2 cells	2, 4, 6, 8, 12 μg/ml	24 h	Apoptosis assay	Alteration in miRNAs synthesis and processing.	Chen et al. (2015)
Other toxicity					
Het-1A cells	1, 2, 4, 8 μg/ml	24 h	Apoptosis assay Cell cycle analysis	Induction of DNA strand breaks and chromosome aberrations. Cell cycle arrest and apoptosis.	Liu et al. (2015)
A549 cells	2, 5, 8 μg/ml	24 h	Apoptosis assay	Induction of apoptosis.	Csepregi et al. (2018)
In vivo Nephrotoxicity					
Mice kidney	0.5, 1, 2, 10, 15, 40 mg/kg/ contaminated diet	26 weeks	Lymphocyte subset analyses	Induction of apoptosis, karyomegaly and tubular degeneration in a dose-dependent manner.	Bondy et al. (2015)

significantly ameliorated oxidative stress, apoptosis and prevented the cell cycle arrest.

3.2.1.1.7. Reproductive toxicity. In this review, OTA-toxicity was also observed in the reproductive system. In testicular cells, TM3 and TM4, a marked decrease in cell proliferation and growth was detected. The down-regulation of PCNA, a typical cell proliferation marker, may explain the significant inhibition of cell cycle progression. In addition, authors obtained the loss of normal physiological functions, failure of spermatogenesis and male infertility due to the marked reduction of calcium concentration in cytosol and mitochondria (Park et al., 2020).

Zhang et al. (2018) investigated the correlation between OTA-exposure and PI3K/PTEN/AMPK signaling pathway activation. Microscopic analysis showed that high doses of OTA significantly increased the expression of PTEN/PI3K, thereby inducing apoptosis and oxidative stress. Whereas, a reduced AKT fluorescent expression can be associated with a reduced motility of spermatozoa *in vitro*.

In summary, anti-PCV2 and 24 h were the most common antibody and exposure time used in IF analysis. The induction of oxidative stress with ROS generation was the main effect related to OTA-administration.

3.2.1.2. In vivo toxicity. Only two *in vivo* OTA-IF studies were found and reviewed. The exposure time ranged between 3 and 6 weeks while doses of 2.50 and 3.50 mg/kg were administered in mice intraperitoneally. No microorganism or natural compounds were tested.

3.2.1.2.1. Nephrotoxicity. With regard to nephrotoxicity *in vivo*, Loboda et al. (2017) demonstrated through the immunostaining of α-SMA, vimentin and collagen I, OTA pro-fibrotic effects while by the fluorescent analysis of caspase 3 and p53, authors confirmed OTA pro-apoptotic activity. Moreover, the immunofluorescent detection of CD45-positive cells indicated higher infiltration of leukocytes and inflammation in mice kidney. Whilst, the reduced fluorescent quantification of HO-1 activity, a cytoprotective enzyme, could promote an additional enhancement in OTA-induced kidney damage. Accordingly, the reduced Nrf2-expression and pro-inflammatory cytokines production, along with HO-1 inhibition, might be considered potential mechanisms involved in OTA-nephrotoxicity.

3.2.1.2.2. Neurotoxicity. As shown in Table 5, fluorescent quantification of astrocytes (GFAP), microglia (Iba) and immature neurons (βIII-Tubulin, Dcx, calretinin) typical markers, revealed both the lack of neuronal differentiation and the reduced presence of astrocytes, microglia and young neurons in the subventricular zone of mice brain. In view of this, OTA-exposure during 6 weeks could affect brain development and neurogenesis, by inducing its neurodegeneration in *in vivo* models (Paradells et al., 2015).

In both *in vivo* studies, a similar dose administration, intraperitoneally, was evidenced.

3.2.2. Flow cytometry

3.2.2.1. In vitro toxicity. *In vitro* OTA FCM-studies were performed using exposure times between 30 min and 40 weeks and doses of 5×10^{-4} – 40 μg/ml. As shown in Fig. 10, the most used cell line was HEK293T. Table 6 points out that various compounds (LUT, SeMet, NAC, TAU, RSV, Zn, CAG, GA, L-Arg, Sil and APS) were implemented to alleviate OTA-toxicity.

3.2.2.1.1. Immunotoxicity. In a time-dependent manner, OTA promoted apoptosis by mitochondria dependent and independent pathways. FCM analysis demonstrated the impairment of cell viability, high percentage of apoptotic necrotic cells (2–20% higher than control cells) and caspase-3 activation. Marked changes in cell morphology and DNA fragmentation were also observed. In addition, OTA triggered the significant modulation of survivin, IL-2 and enhanced the autocrine pro-apoptotic effect of TNF-α (Darif et al., 2016).

In human neutrophils, OTA mediated the release of calcium from

internal stores, causing oxidative burst, ATP depletion and MMP disturbance. As mitochondria play a key role in cell vitality, their disruption led to apoptosis in a dose and time depended manner. At the same time, the biodegradation of OTA into its metabolite, OTA-α, by gastrointestinal microorganisms, could be a promising strategy to alleviate OTA-immunotoxicity (Kupski et al., 2016). In alveolar macrophages, OTA-administration promoted both nuclear condensation and apoptotic bodies formation with alterations in caspase 3/9 expression and cytokines production. In contrast, high doses of APS could attenuate the immune stress induced by OTA via AMPK/SIRT-1 signaling pathway (Liu et al., 2018). In the same *in vitro* model, 48 h exposure to toxin significantly caused cell death and intracellular ROS generation in a dose-dependent manner. Also, OTA may enhance the phosphorylation of ERK1/2, p38, and NF-κB p65 pathways, thereby increasing the production of pro-inflammatory cytokines. However, high doses of NAC reversed OTA-induced apoptosis, oxidative stress and inflammation (Xu et al., 2017).

Regarding long lasting exposure, the association between OTA and autoimmune diseases such as rheumatoid arthritis (RA) was analyzed. The release of pro-inflammatory cytokines, IL-1β, IL-6 and TNF-α, in macrophages was markedly observed after low levels of OTA-exposure. In addition, this mycotoxin increased the susceptibility to develop RA via Th1/Th17 cell differentiation and STAT signaling pathway activation (Jahreis et al., 2017).

3.2.2.1.2. Hepatotoxicity. In HepG2 cells, exposure to different concentrations of OTA reduced both protein synthesis and intracellular ATP content in a dose-dependent manner. Moreover, it induced cell death with a marked disorganization of intracellular structures, especially in actin filaments of cytoskeleton (Sali et al., 2016).

As shown in Table 6, in chicken hepatocytes, the promotion of oxidative stress, lipid peroxidation with suppressed SOD and GSH activities were detected upon 24 h OTA-contamination. It also increased cell death and caspase-3 activity, suggesting the association between apoptosis and mitochondrial dysfunctions. The pre-treatment with CAG, L-Arg, Sil and GA could protect the liver by alleviating OTA-induced oxidative stress and apoptosis (Yu et al., 2018).

Zhu et al. (2016) suggested that cell death is the primary MOA in OTA-induced hepatotoxicity while miR-122 is the primary effector of apoptosis via CCNG1/p53 and Bcl/caspase-3 pathways activation. As confirmation of this hypothesis, the treatment with hsa-miR-122 inhibitor significatively reversed OTA-toxic effects. In rat liver cells, FCM analysis demonstrated the positive association between cell death and OTA-exposure. In this case, the expression of typical apoptotic proteins was significantly altered (Wang et al., 2020). In HepG2 cells, Juan-García et al. (2019) observed by FCM analysis the G_0/G_1 cell cycle arrest with DNA damage upon 48 h OTA-contamination.

3.2.2.1.3. Gastrointestinal toxicity. In IPEC-J2 cells, OTA-exposure caused typical apoptotic changes in the nucleus and promoted cell death in a time-dependent manner. Also, it triggered mitochondrial dysfunctions with ROS production, cyt-c release and caspase-3 activation. However, ERK1/2 pathway activation alleviated OTA-damage, by protecting the integrity of intestinal barrier (Wang et al., 2018). Similarly, in the same cell line, mitochondrial ROS generation, cyt-c release and caspase-3 activation were observed upon 12 h toxin-exposure. Nevertheless, Mito-TEMPO, a mitochondria-targeted ROS-scavenger, played a protective role against oxidative stress and mitochondrial dysfunctions (Wang et al., 2017).

Li et al. (2019), in GES-1 cells, analyzed the involvement of mitochondria in OTA-MOA. Authors detected the promotion of oxidative stress, apoptosis and mitochondrial disturbances with MMP loss and ATP depletion. At the same time, OTA enhanced AMPK activation and up-regulated PGC-1α, NRF-1 and TFAM factors, by stimulating the biogenesis of new mitochondria, which might be a cellular response to damaging agents.

Interestingly, Yang et al. (2019) suggested that the impairment of small intestine, the main site of OTA-absorption, might be partly attributed to apoptosis, which was associated in turn with the loop interaction between MDM2 and p53 signaling pathway. OTA suppressed MDM2 expression and led to cell death through CASP3 activation and its downstream pattern.

In gastric cells, chronic exposure to OTA (3 days of toxin-exposure each week during 40 weeks) caused malignant transformations via Wnt/β-catenin pathway activation. FCM analysis confirmed the increased rate of cells in the proliferative stage (phases G_2/M and S) and the intracellular ROS generation. High concentration of NAC could mitigate the long-term OTA-toxicity confirming its excellent antioxidant capacity (Jia et al., 2016).

3.2.2.1.4. Nephrotoxicity. FCM-analysis conducted by Agarwal et al. (2020) revealed that OTA triggered intracellular ROS generation and cell cycle arrest at phase S and G_0 in a time linked spiral response. In addition, the promotion of cell death and mitochondrial impairment with MMP loss was significantly observed. In contrast, NAT largely ameliorated OTA-mediated oxidative stress, cell cycle dysregulation, MMP destabilization and cell death. It has been demonstrated NAT-capacity to compete with OTA binding-pocket on phenylalanyl t-RNA synthetase, by preventing eventual alterations in protein synthesis.

In NRK-52 E cells, exposure to toxin increased intracellular ROS production, lipid peroxidation with a reduced activity of antioxidant enzymes (SOD and GSH). Pre-treatment with LUT effectively neutralized ROS production and oxidative stress owing to its ROS-scavenging capacities (Liu et al., 2020).

Furthermore, OTA-nephrotoxicity might be promoted by apoptosis signal-regulating kinase 1 (ASK1) activation. ASK-1, a mitogen-activated protein kinase kinase kinase (MAPKKK, MAP3K), is activated by OTA and promoted ROS generation, apoptosis and mitochondrial dysfunctions. Nevertheless, these toxicological effects could be reversed by ASK-1 knockdown, indicating its clear involvement in OTA-induced kidney injury (Liang et al., 2015).

As shown in Table 6, OTA may induce a global alteration of DNA methylation, leading to a hypermethylation of essential genes associated with G_1/S phase transition, G_1/DNA damage checkpoints signal transduction and anaphase-promoting complex/cyclosome protein. Consequently, OTA-triggered G_0/G_1 cell cycle arrest was observed (Zhang et al., 2020).

Exposure to OTA, alone or in combination with ZEA, promoted cell death by altering Bax, Bcl-2, and caspase-3 expression. However, a novel mode to suppress toxins activity has been proposed. A recombinant fusion enzyme (ZHDCP), by combining two single genes, zearalenone hydrolase and carboxypeptidase, suppressed OTA and ZEA-cytotoxicity, degrading them with 100% efficiency (Azam et al., 2019).

In the 24 h study, OTA impaired the expression of organic cation transport 1, 2, 3 (OCT1, OCT2 and OCT3) and induced cell death via mitochondrial pathway. Additionally, ROS generation and DNA damage were detected. However, OCT-2 knockout and TEA-treatment, a specific OCT-2 inhibitor, significantly improved OTA-mediated cell death, oxidative stress and DNA damage *in vitro* (Qi et al., 2018). Another toxicological mechanism whereby OTA induced kidney toxicity was the induction of pyroptosis, a novel mechanism of programmed cell death. Indeed, OTA promoted the activation of NLRP3 inflammasome complex, which in turn activated caspase 1. This enzyme cleaved the precursors of inflammatory cytokines, IL-18 and IL-1β, by inducing the inflammatory response in neighboring cells (Li et al., 2021).

In MDCK cells, OTA induced apoptosis and oxidative stress by altering the expression of metallothionein-1 (MT-1) and metallothionein-2 (MT-2). Nevertheless, MTs, a group of small cysteine-rich proteins known for its strong free scavenging and antioxidant capacity, were up-regulated by zinc supplementation, thereby reversing intracellular ROS production and cell death (Li et al., 2019). Similarly, RSV confirmed its potential anti-oxidant and chemo-preventive proprieties by suppressing oxidative stress and DNA damage induced by OTA-administration (Raghubeer et al., 2015).

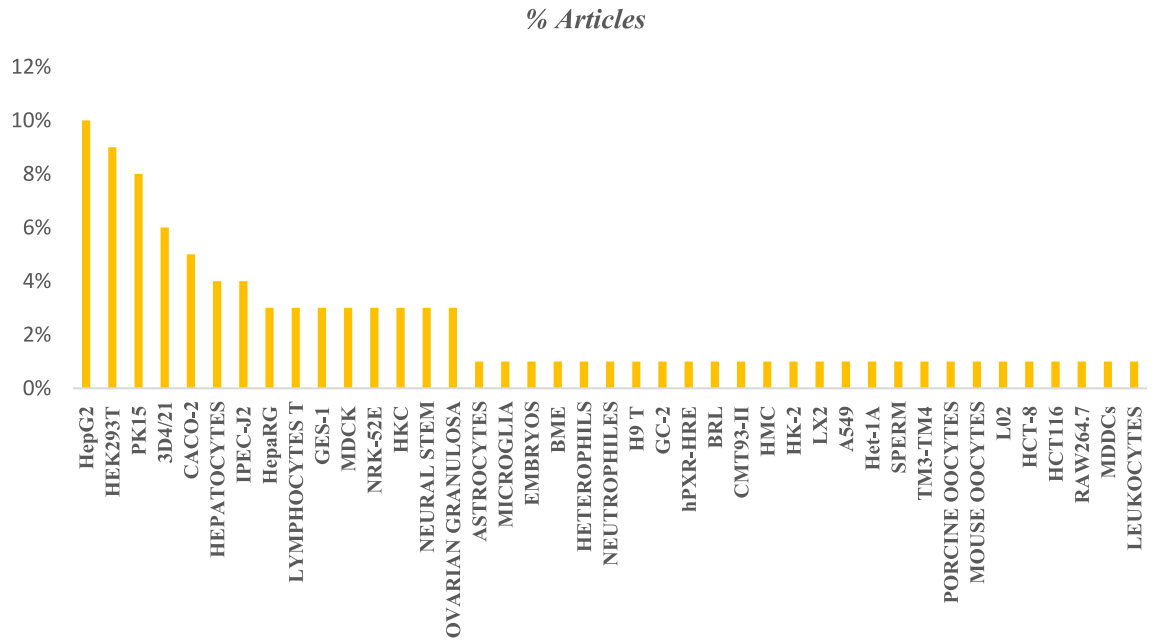

Fig. 11. Percentage of studies according to the main cell lines employed.

Gong et al. (2019) showed the involvement of microRNAs (miRNAs) in OTA-promoted nephrotoxicity. Indeed, hsa-miR-1-3p and hsa-miR-122–5p played an important role in the induction of apoptosis and cell cycle arrest by regulating the expression of their target genes, programmed cell death 10 and cyclin G1, respectively.

In HK-2 cell line, the cell cycle arrest was related to cyclin-dependent kinase 2 (CDK2). This kinase was downregulated by OTA exposure while its overexpression partially blocked OTA-mediated G_1 cell cycle arrest. In view of this, CDK2 can be considered one of the key regulators of G_1 cell cycle arrest promoted by low concentrations of OTA (Dubourg et al., 2020).

In relation to PK15 cell line, 48 h exposure to OTA significantly promoted cell death and oxidative stress with a reduction of GSH content (20% less than control cells) and an increase ROS and oxidants production. NAC-treatment significantly abrogated ROS production and oxidative stress by improving cell antioxidant defenses (Gan et al., 2015a; Qian et al., 2017). Furthermore, Liu et al. (2020) associated the high apoptotic rate with the altered expression of Bax, caspase-3 and Bcl-2. In this study, taurine-supplementation alleviated cell death by restoring the expression of apoptosis-related proteins to the control level. In a similar way, SeMet could alleviate OTA-induced kidney damage, apoptosis and oxidative stress by improving selenoenzyme expression and by restoring Gpx activity (Gan et al., 2015b).

3.2.2.1.5. Embryotoxicity. As reported in Table 6, only two studies were reviewed. Zhang et al. (2019) observed that OTA-exposure compromised ovarian GCs viability in a concentration-dependent manner, by inducing late apoptosis/necrosis with oxidative stress and ROS generation. In addition, a positive correlation between cell death and PI3K/AKT signaling pathway was observed. By reducing the ratio of p-AKT/AKT, OTA led to a dysregulation of apoptosis-related genes, Bax and caspase 9, and consequently a high percentage of apoptotic cells.

Zhang et al. (2020) observed the clear arrest of cell cycle at G_2/M stage with the reduction of DNA content in a dose-dependent manner. These findings were closely associated with DNA damage and dysregulation of DNA-repair processes promoted by OTA-administration.

3.2.2.1.6. Reproductive toxicity. As mentioned above, Park et al. (2020) revealed that OTA was capable to promote a significant decrease in the proliferative rate of TM3 and TM4 cell lines. Also, toxin reduced the concentration of calcium ions in the cytosol and mitochondria, by disrupting both cellular homeostasis and physiological functions. FCM analysis showed a high percentage of cells in the sub-G_1 stage, indicating a cell cycle arrest at phase G_0/G_1. The antiproliferative effects of OTA were related to PI3K and MAPK signaling pathways.

As shown in Table 6, high doses of OTA significantly decreased sperm motility *in vitro* via PTEN/AMPK pathway activation. As expected, OTA increased intracellular ROS generation and triggered cell death by altering p53 and Bax expression. Nevertheless, neither the vitality nor mitochondrial functions were altered by OTA-exposure (Zhang et al., 2018). Finally, the role of miRNAs in OTA-reproductive toxicity was examined. In germ cells, it has been demonstrated that several pathways involved in cell proliferation and differentiation were dysregulated. Moreover, the high percentage of apoptotic cells, associated with p53 and caspase-3 pathways, was partly mediated by miR-122 activation (Chen et al., 2015).

3.2.2.1.7. Other toxicity. Finally, OTA-detrimental effects have been also studied in esophageal and lung cells. In a 24 h study, exposure to toxin caused DNA damage and chromosome aberrations in Het-1A cells. DNA damage was followed by G_2 cell cycle arrest, with the down-regulation of Cdc2 and cyclin B1 expression. In this study, the cell death was related to mitochondrial dysfunctions (Liu et al., 2015). Whereas, in A549 cells, it has been confirmed that apoptosis is one of the main OTA-MOA to induce lung toxicity (Csepregi et al., 2018).

To sum up, 24 h and apoptosis assay were the most common exposure time and assay used. The promotion of apoptosis and ROS generation were the main toxicological effects obtained upon OTA-administration.

3.2.2.2. In vivo toxicity. As regards *in vivo* toxicity, only one study was reported. It was performed during 26 weeks on mice with concentrations ranged between 0.5 and 40 mg/kg administered in contaminated diet. No natural compounds were tested to counteract OTA-effects (Table 6).

3.2.2.2.1. Nephrotoxicity. In kidney, the transcriptional regulator p53 triggers DNA damage repair processes and reverses cell cycle arrest due to the activation of cell-cycle checkpoints. Chronic exposure to OTA in p53 heterozygous ($p53^{+/-}$) and homozygous ($p53^{+/+}$) mice, provoked kidney injury with alterations in cell proliferation, apoptosis and tubular degeneration in a dose-dependent manner (Bondy et al., 2015).

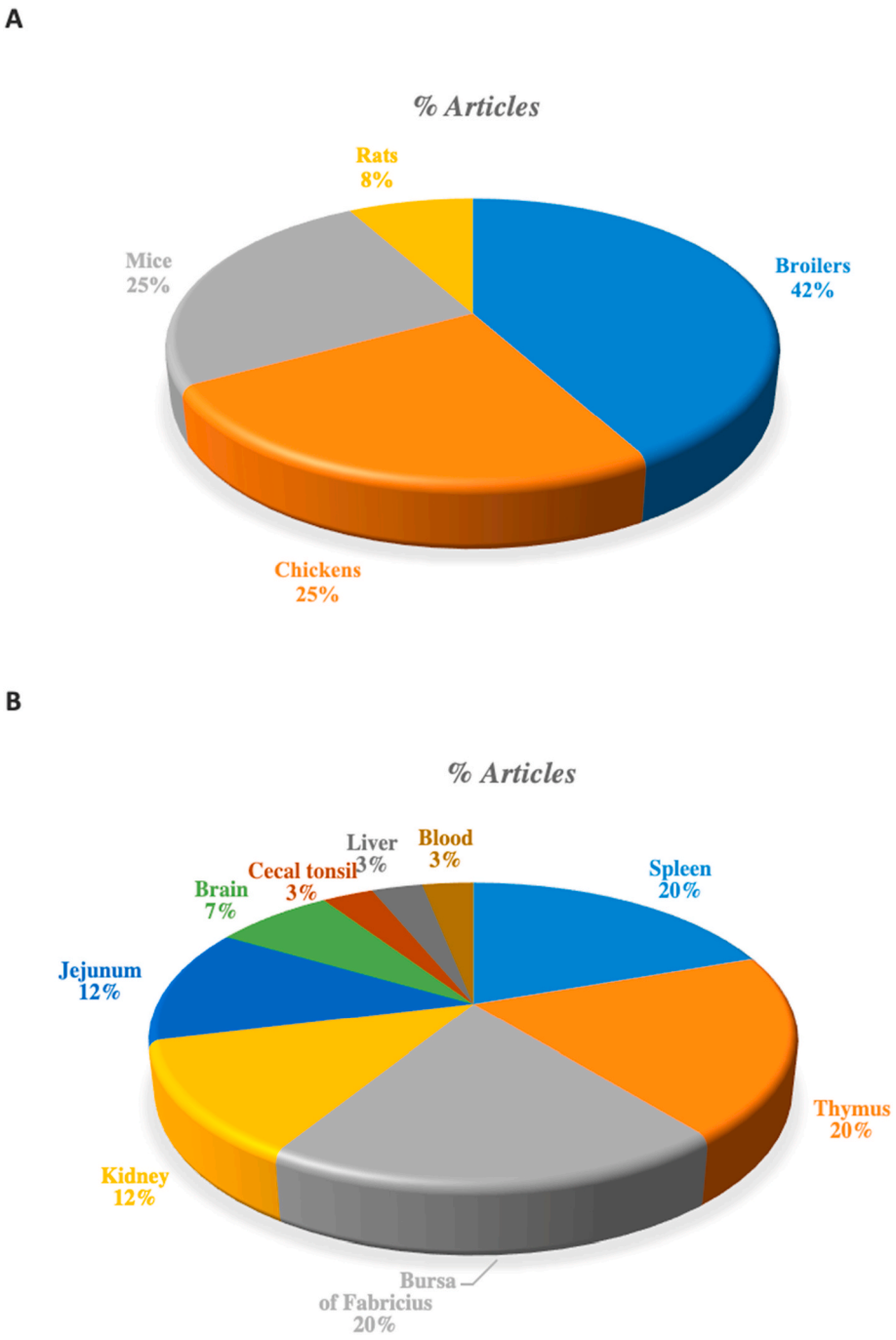

Fig. 12. A. Percentage of studies according to the animal species. **B.** Percentage of studies according to the organ studied.

4. Discussion

Analyzing all the studies reviewed in this work, it emerges that the most used cell lines were HepG2 (10%), HEK-293T (9%), PK15 (8%), 3D4/21 (6%), Caco-2 (5%), hepatocytes and IPEC-J2 cell line (4%). A similar percentage is constituted by HepaRG, human lymphocytes, GES-1, MDCK, NRK-52E, HKC, neural stem and porcine ovarian granulosa cells (3%). The less frequent were astrocytes, microglia, porcine embryos, BME cells, heterophils, neutrophils, H9-T, GC-2, hPXR-HRE, BRL, CMT93-II, HMC, HK-2,LX2, A549, Het-1A, sperm and TM3-TM4 cells, porcine and mouse oocytes, L02, HCT-8, HCT116, RAW264.7, MDDCs cells and leukocytes (1%) (Fig. 11).

Regarding the use of laboratory animals in the studies, the main specie used was broilers (42%), followed by mice (25%), chickens (25%) and rats (8%) (Fig. 12A). The main targeted organs used were thymus, BF and spleen (20%), followed by jejunum and kidney (12%). A smaller percentage included the use of brain (7%), tonsil, liver and blood/plasma analysis (3%) (Fig. 12B).

As shown in Fig. 13, the most common purpose of the studies was immunotoxicity (29%), followed by nephrotoxicity (24%), hepatotoxicity (16%), gastrointestinal toxicity (14%). Less frequent were the studies of neurotoxicity (6%), embryotoxicity (5%), reproductive system (2%), breast, esophageal and lung toxicity (1%).

In relation to IF staining, the antibodies were selected depending on the specific route or biological processes searched by authors, in order to clarify AFB1 and OTA-MOA. Therefore, anti-γH2AX (40%), anti-8OHdG, anti-ATR, anti-CRM1, anti-PCNA, anti-Rad51 and anti-Brca1 (10%) were implemented to reveal DNA damage (Fig. 14A). To assess AFB1

Fig. 13. Percentage of articles (n = 98) according to the main purpose of the study.

and OTA ability to promote viral replication, anti-PCV2 (60%), anti-EBNA-2 and anti-NP (20%) were employed (Fig. 14B). Whilst, inflammation was detected through anti-p65 (34%), anti-CD45 (14%), anti-CD20, anti-RIP3, anti-NF-kB and anti-NLRP3 (13%) (Fig. 14C). Moreover, anti-elastase and anti-histone H3 (34%) anti-eDNA and anti-MPO (16%) were used to identified ETs formation (Fig. 14D) while anti-DNMT1, anti-H3K9ac and anti-H3K9me3 (33%) to confirm epigenetic modifications (Fig. 14E). Several antibodies were also utilized to evaluate neural differentiation: anti-GFAP (19%), anti-Dcx (11%), anti-mGalc, anti-calretinin, anti-Iba1, anti-NeuN, anti-MAP2-AP18/M13, anti-βIII- Tubulin, anti-Nestin and anti-A2B5 (8%) (Fig. 14F). Furthermore, anti-α tubulin (41%), anti-vimentin (25%) anti-collagen I and anti-α SMA (17%) were used to assess fibrosis and cell integrity (Fig. 14G) whereas anti-claudin-4 (28%), anti-claudin-3 (17%), anti-occludin, anti-ZO1, anti-β-catenin, anti-claudin-6, anti-claudin-2 (11%) to investigate intestinal barrier integrity (Fig. 14H). Metabolic routes involved in AFB1 and OTA-MOA were detected by anti-ERK1/2, anti-AKT, anti-PTEN and anti-PI3K (25%) (Fig. 14I). Regarding the oxidative stress and hypoxia, anti-Arg1, anti-iNOS, anti-HIF-1α, anti-NRF2, anti-HO-1 and anti-Gpx (14%) were employed (Fig. 14L). Whilst, anti-p53BP1 (34%), anti-Bax, anti-Bcl-2, anti-caspase-3, anti-cyt C and anti-GSDMD (13%) were used to reveal cell death (Fig. 14M). Moreover, Beclin-1 (33%) and LC3 (67%) were implemented to detect autophagy while Kim-1 and Grp75 (50%) to identify kidney injury. Finally, embryogenesis (anti-ITGB1), thrombosis (anti-F2R), specific epitope identification (anti-FLAG), AFB1-DNA adduct formation (anti-AFB1) and mitochondrial import process (anti-TOM20) were also investigated.

As regard FCM technique, the most common analysis was apoptosis assay (41%), followed by cell cycle analysis (21%) and ROS measurement (15%). A smaller percentage was constituted by immune cell subset analysis and MMP measurement (4%) and DNA damage analysis (3%), T cells identification, intracellular/mitochondrial calcium determination and AFB1-DNA adduct formation (2%). The less used were TH1/TH17 analysis, Caspase 1/3 detection, intracellular oxidants assay, cell viability assay, immune markers and cytokine evaluation, FOXP3 determination, cancer cells quantification, phagocytes assay and mitochondrial mass determination (1%) (Fig. 15).

With regard to AFB1, *in vitro* IF-studies showed that 24 h and anti-γH2AX were the most common exposure time and antibody used. The induction of oxidative stress with ROS generation and apoptosis were the main toxicological effects detected. For *in vivo* studies, a similar exposure time (8 weeks) was observed. As regards *in vitro* AFB1-FCM studies, 24 h and 48 h were the most common exposure times while the apoptosis assay was the main analysis performed. The promotion of apoptosis and cell cycle arrest were the main toxicological damages observed. *In vivo* studies, 3 weeks was the main exposure time while the apoptosis assay was mostly performed. The enhancement of apoptosis, cell cycle arrest and immunosuppression were mainly detected.

In relation to OTA, *in vitro* IF-studies evidenced that anti-PCV2 and 24 h were the most common antibody and exposure time used. The induction of oxidative stress was the main effect related to OTA-administration. *In vivo* studies showed a similar dose administration (intraperitoneally). As regards *in vitro* OTA-FCM studies, 24 h and apoptosis assay were the most common exposure time and assay employed. As expected, the promotion of apoptosis and ROS generation were the main toxicological damages detected. Whilst, *in vivo*, only one study was screened. It has been performed during 26 weeks in mice with high doses of OTA, which were supplied in contaminated feed.

5. Conclusions

In the last six years, in the study of AFB1- and OTA-toxicity by IF and FCM techniques, the most used cell line was HepG2, followed by HEK-293T, PK15, 3D4/21, Caco-2, hepatocytes, IPEC-J2, HepaRG, human lymphocytes, GES-1, MDCK, NRK-52E, HKC, neural stem and porcine ovarian granulosa cells. In *in vivo* studies, the predominant laboratory animals employed were broilers followed by mice, chickens and rats while the main targeted organs used were thymus, BF, and spleen. The main purpose of the researches was immunotoxicity, followed by nephrotoxicity, hepatotoxicity, gastrointestinal toxicity, neurotoxicity, embryotoxicity, reproductive system, breast, esophageal and lung toxicity. The effect of several compounds to counteract AFB1- and OTA-toxicological damages was also investigated.

Regarding the IF analysis, different antibodies were employed to elucidate alterations in various biological process related to AFB1- and OTA-toxicity such as: DNA, cell and intestinal integrity, inflammation, neural differentiation, oxidative stress and cell death. Whilst, in FCM analysis, several assays were performed. The predominant were the apoptosis assay, cell cycle analysis and intracellular ROS measurement.

In conclusion, the present work confirms the toxicity of AFB1 and OTA and their potential harmful effects on *in vitro* and *in vivo* models. Nevertheless, the high number of *in vitro* studies and the scarceness of *in vivo* researches can be clearly discerned. In relation to OTA, only two studies were reviewed, indicating the lack of information obtained by FCM and IF in the last six years. Regarding AFB1, very scarce sources were found for neurotoxicity, nephrotoxicity and hepatotoxicity.

In view of this, more *in vivo* trials are needed to provide a more extensive and precise overview on AFB1- and OTA-toxicity and their MOA on human health.

Conflicts of interest

Authors declare no have conflicts of interest.

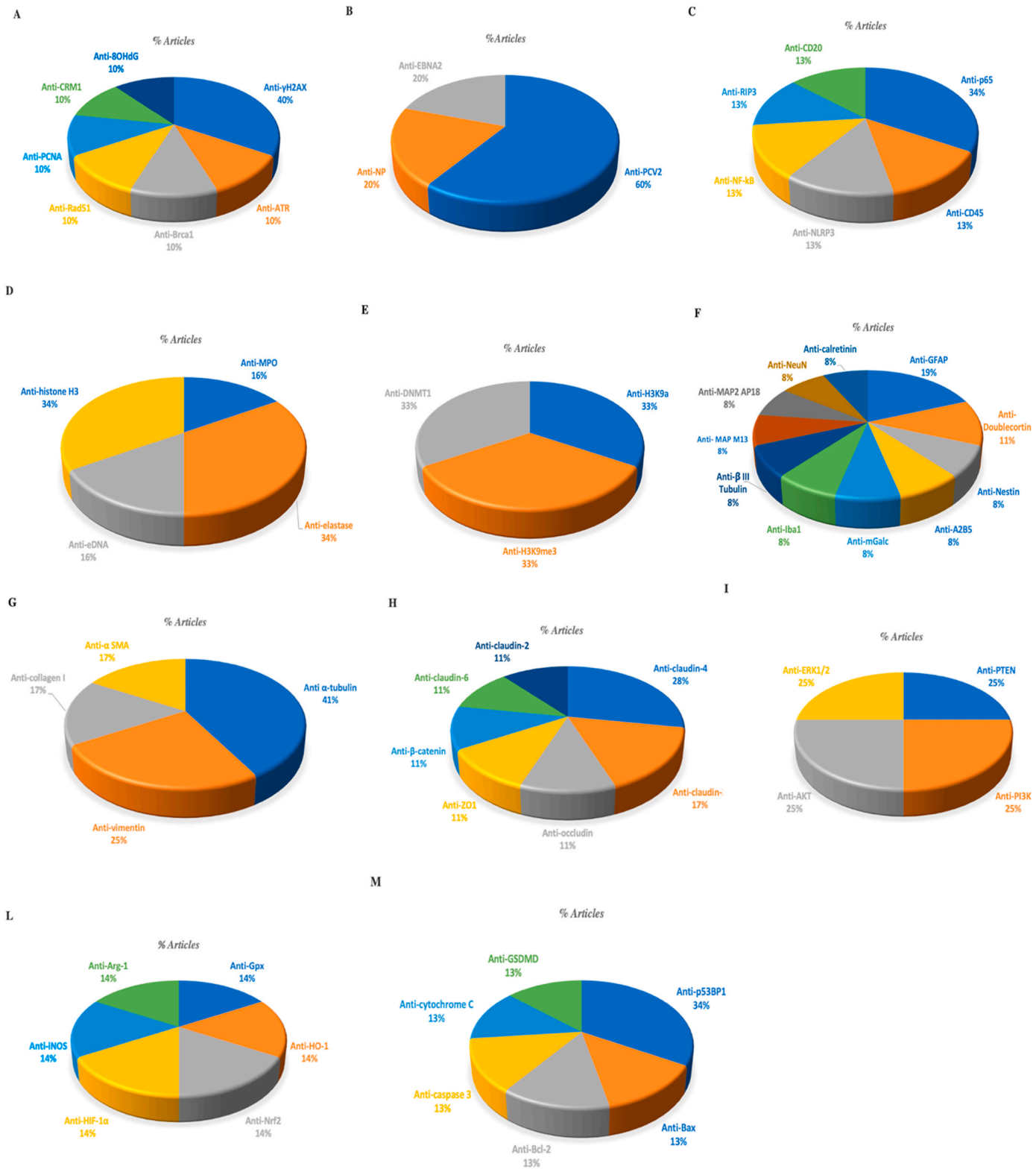

Fig. 14. Pie charts of antibodies used in the reviewed studies. **A.** Pie chart of antibodies related to DNA damage in the revised papers. **B.** Pie chart of antibodies related to viral replication in the revised articles. **C.** Pie chart of antibodies related to inflammation in the revised publications. **D.** Pie chart of antibodies related to extracellular traps in the revised papers. **E.** Pie chart of antibodies related to epigenetic modifications in the revised articles. **F.** Pie chart of antibodies related to neural differentiation in the revised publications. **G.** Pie chart of antibodies related to cell integrity in the revised papers. **H.** Pie chart of antibodies related to intestinal barrier integrity in the revised articles. **I.** Pie chart of antibodies used to detect metabolic route in the revised publications. **L.** Pie chart of antibodies related to oxidative stress and hypoxia in the revised papers. **M.** Pie chart of antibodies related to cell death in the revised articles.

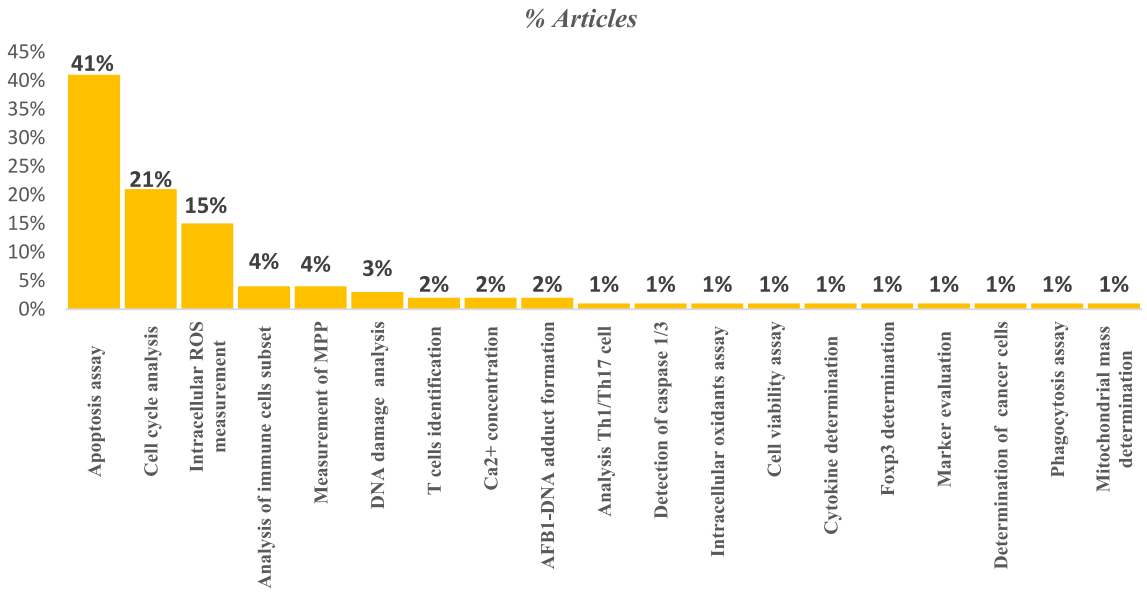

Fig. 15. Percentage of FCM assays employed in the reviewed studies.

CRediT authorship contribution statement

Massimo Frangiamone: Visualization, Writing – original draft. **Alessandra Cimbalo:** Visualization, Writing – original draft. **Manuel Alonso-Garrido:** Writing – original draft, Writing – review & editing. **Pilar Vila-Donat:** Writing – review & editing. **Lara Manyes:** Funding acquisition, Project administration, Supervision, Writing – review & editing.

Declaration of competing interest

The authors declare that they have no known competing financial interests or personal relationships that could have appeared to influence the work reported in this paper.

Acknowledgements

This work was supported by the Spanish Ministry of Science and Innovation (PID2019-108070RB-I00-ALI). AC wishes to thank the Generalitat Valenciana (PROMETEO/2018/126) and MAG to Spanish Ministry of Science and Innovation (BES-2017-081328) for the PhD grants.

References

Abbès, S., Ben Salah-Abbes, J., Jebali, R., Younes, R.B., Oueslati, R., 2016. Interaction of aflatoxin B1 and fumonisin B1 in mice causes immunotoxicity and oxidative stress: possible protective role using lactic acid bacteria. J. Immunot. 13 https://doi.org/10.3109/1547691X.2014.997905.

Accardi, R., Gruffat, H., Sirand, C., Fusil, F., Gheit, T., Hernandez-Vargas, H., Le Calvez-Kelm, F., Traverse-Glehen, A., Cosset, F.L., Manet, E., Wild, C.P., Tommasino, M., 2015. The mycotoxin aflatoxin B1 stimulates Epstein–Barr virus-induced B-cell transformation in in vitro and in vivo experimental models. Carcinogenesis 36, 1440–1451. https://doi.org/10.1093/carcin/bgv142.

Agarwal, P., Singh, D., Raisuddin, S., Kumar, R., 2020. Amelioration of ochratoxin-A induced cytotoxicity by prophylactic treatment of N-Acetyl-L-Tryptophan in human embryonic kidney cells. Toxicology 429, 152324. https://doi.org/10.1016/j.tox.2019.152324.

Alsayyah, A., ElMazoudy, R., Al-Namshan, M., Al-Jafary, M., Alaqeel, N., 2019. Chronic neurodegeneration by aflatoxin B1 depends on alterations of brain enzyme activity and immunoexpression of astrocyte in male rats. Ecotoxicol. Environ. Saf. 182, 109407. https://doi.org/10.1016/j.ecoenv.2019.109407.

Alshannaq, A., Yu, J.H., 2017. Occurrence, toxicity, and analysis of major mycotoxins in food. Int. J. Environ. Res. Publ. Health 14, 632. https://doi.org/10.3390/ijerph14060632.

An, Y., Shi, X., Tang, X., Wang, Y., Shen, F., Zhang, Q., Wang, C., Jiang, M., Liu, M., Yu, L., 2017. Aflatoxin B1 induces reactive oxygen species-mediated autophagy and extracellular trap formation in macrophages. Front. Cell. Inf. Microbiol. 7, 53. https://doi.org/10.3389/fcimb.2017.00053.

Anfossi, L., Giovannoli, C., Baggiani, C., 2016. Mycotoxin detection. COBIOT 37, 120–126. https://doi.org/10.1016/j.copbio.2015.11.005.

Ayofemi Olalekan Adeyeye, S., 2020. Aflatoxigenic fungi and mycotoxins in food: a review. Crit. Rev. Food Sci. Nutr. 60, 709–721. https://doi.org/10.1080/10408398.2018.1548429.

Azam, M.S., Yu, D., Liu, N., Wu, A., 2019. Degrading ochratoxin A and zearalenone mycotoxins using a multifunctional recombinant enzyme. Toxins 11, 301. https://doi.org/10.3390/toxins11050301.

Babayan, N., Tadevosyan, G., Khondkaryan, L., Grigoryan, R., Sarkisyan, N., Haroutiounian, R., Stopper, H., 2020. Ochratoxin A induces global DNA hypomethylation and oxidative stress in neuronal cells in vitro. Mycotoxin Res. 36, 73–81. https://doi.org/10.1007/s12550-019-00370-y.

Bahey, N.G., Abd Elaziz, H.O., Gadalla, K.K.E.S., 2015. Toxic effect of aflatoxin B1 and the role of recovery on the rat cerebral cortex and hippocampus. Tissue Cell 47, 559–566. https://doi.org/10.1016/j.tice.2015.09.001.

Bakheet, S.A., Attia, S.M., Alwetaid, M.Y., Ansari, M.A., Zoheir, K.M., Nadeem, A., Al-Shabanah, O.A., Al-Harbi, M.M., Ahmad, S.F., 2016. β-1, 3-Glucan reverses aflatoxin B1-mediated suppression of immune responses in mice. Life Sci. 152, 1–13. https://doi.org/10.1016/j.lfs.2016.03.030.

Ben Salah-Abbes, J., Jebali, R., Sharafi, H., Akbari Noghabi, K., Oueslati, R., Abbès, S., 2016. Immuno-physiological alterations from AFB1 in rats counteracted by treatments with Lactobacillus paracasei BEJ01 and montmorillonite clay mixture. J. Immunot. 13, 628–637. https://doi.org/10.3109/1547691X.2016.1145157.

Benkerroum, N., 2020. Chronic and acute toxicities of aflatoxins: mechanisms of action. Int. J. Environ. Res. Publ. Health 17, 423. https://doi.org/10.3390/ijerph17020423.

Bernáldez, V., Cordoba, J.J., Magan, N., Peromingo, B., Rodríguez, A., 2017. The influence of ecophysiological factors on growth, aflR gene expression and aflatoxin B1 production by a type strain of Aspergillus flavus. LWT-Food Sci. Technol. 83, 283–291. https://doi.org/10.1016/j.lwt.2017.05.030.

Bertero, A., Moretti, A., Spicer, L.J., Caloni, F., 2018. Fusarium molds and mycotoxins: potential species-specific effects. Toxins 10, 244. https://doi.org/10.3390/toxins10060244.

Bhat, P.V., Pandareesh, M.D., Khanum, F., Tamatam, A., 2016. Cytotoxic effects of ochratoxin A in neuro-2a cells: role of oxidative stress evidenced by N-acetylcysteine. Front. Microbiol. 7, 1142. https://doi.org/10.3389/fmicb.2016.01142.

Bleichrodt, R.J., Read, N.D., 2019. Flow cytometry and FACS applied to filamentous fungi. Fungal Biol. Rev. 33, 1–15. https://doi.org/10.1016/j.fbr.2018.06.001.

Bondy, G.S., Caldwell, D.S., Aziz, S.A., Coady, L.C., Armstrong, C.L., Curran, I.H., Koffman, R.L., Kapal, K., Lefebvre, D.E., Mehta, R., 2015. Effects of chronic ochratoxin A exposure on p53 heterozygous and p53 homozygous mice. Toxicol. Pathol. 43, 715–729. https://doi.org/10.1177/0192623314568391.

Bryła, M., Waśkiewicz, A., Ksieniewicz-Woźniak, E., Szymczyk, K., Jędrzejczak, R., 2018. Modified fusarium mycotoxins in cereals and their products—metabolism, occurrence, and toxicity: an updated review. Molecules 23, 963. https://doi.org/10.3390/molecules23040963.

Broemsen, E.L., Place, A.R., Parrow, M.W., 2021. Quantitative nuclear DNA content and cell cycle analysis of a mixotrophic dinoflagellate by image cytometry. Limnol Oceanogr. Methods 19, 253–266. https://doi.org/10.1002/lom3.10420.

Chen, J., Chen, K., Yuan, S., Peng, X., Fang, J., Wang, F., Cui, H., Chen, Z., Yuan, J., Geng, Y.E., 2016. Effects of aflatoxin B1 on oxidative stress markers and apoptosis of spleens in broilers. Toxicol. Ind. Health 32, 278–284. https://doi.org/10.1177/0748233713500819.

Chen, R., Deng, L., Yu, X., Wang, X., Zhu, L., Yu, T., Luo, H., Zhang, Y., Zhou, B., Xu, W., Chen, L., Luo, H., 2015. MiR-122 partly mediates the ochratoxin A-induced GC-2 cell apoptosis. Toxicol. Vitro 30, 264–273. https://doi.org/10.1016/j.tiv.2015.10.011.
Chen, W., Li, C., Zhang, B., Zhou, Z., Shen, Y., Liao, X., Yang, J., Wang, Y., Li, X., Li, Y., Shen, X.L., 2018. Advances in biodetoxification of ochratoxin A. A review of the past five decades. Front. Microbiol. 9, 1386. https://doi.org/10.3389/fmicb.2018.01386.
Chen, Y.Y., Lin, Y., Han, P.Y., Jiang, S., Che, L., He, C.Y., Lin, Y.C., Lin, Z.N., 2019. HBx combined with AFB1 triggers hepatic steatosis via COX-2-mediated necrosome formation and mitochondrial dynamics disorder. J. Cell Mol. Med. 23, 5920–5933. https://doi.org/10.1111/jcmm.14388.
Cimbalo, A., Alonso-Garrido, M., Font, G., Manyes, L., 2020. Toxicity of mycotoxins in vivo on vertebrate organisms: a review. Food Chem. Toxicol. 137, 111161 https://doi.org/10.1016/j.fct.2020.111161.
Csepregi, R., Temesfői, V., Poór, M., Faust, Z., Kőszegi, T., 2018. Green fluorescent protein-based viability assay in a multiparametric configuration. Molecules 23, 1575. https://doi.org/10.3390/molecules23071575.
Dai, Y., Huang, K., Zhang, B., Zhu, L., Xu, W., 2017. Aflatoxin B1-induced epigenetic alterations: an overview. Food Chem. Toxicol. 109, 683–689. https://doi.org/10.1016/j.fct.2017.06.034.
Darif, Y., Mountassif, D., Belkebir, A., Zaid, Y., Basu, K., Mourad, W., Oudghiri, M., 2016. Ochratoxin A mediates MAPK activation, modulates IL-2 and TNF-α mRNA expression and induces apoptosis by mitochondria-dependent and mitochondria-independent pathways in human H9 T cells. J. Toxicol. Sci. 41, 403–416. https://doi.org/10.2131/jts.41.403.
Du, M., Liu, Y., Zhang, G., 2017. Interaction of aflatoxin B1 and fumonisin B1 in HepG2 cell apoptosis. Food Biosci. 20, 131–140. https://doi.org/10.1016/j.fbio.2017.09.003.
Dubourg, V., Nolze, A., Kopf, M., Gekle, M., Schwerdt, G., 2020. Weighted Correlation Network Analysis Reveals CDK2 as a regulator of a ubiquitous environmental toxin-induced cell-cycle arrest. Cells 9, 143. https://doi.org/10.3390/cells9010143.
European Commission, 2006. Commission Regulation (EC) No 1881/2006 of 19 December 2006 setting maximum levels for certain contaminants in foodstuffs. Off. J. EU. 364, 365–324. https://eurlex.europa.eu/LexUriServ/LexUriServ.do?uri=OJ:L:2006:364:0005:0024.
Eskola, M., Kos, G., Elliott, C.T., Hajšlová, J., Mayar, S., Krska, R., 2020. Worldwide contamination of food-crops with mycotoxins: validity of the widely cited 'FAO estimate'of 25. Crit. Rev. Food Sci. Nutr. 60, 2773–2789. https://doi.org/10.1080/10408398.2019.1658570.
Fang, J., Yin, H., Zheng, Z., Zhu, P., Peng, X., Zuo, Z., Cui, H., Zhou, Y., Ouyang, P., Geng, Y., Deng, J., 2018. The molecular mechanisms of protective role of Se on the G 2/M phase Arrest of jejunum caused by AFB 1. Biol. Trace Elem. Res. 181, 142–153. https://doi.org/10.1007/s12011-017-1030-2.
Fang, J., Zhu, P., Yang, Z., Peng, X., Zuo, Z., Cui, H., Ouyang, P., Shu, G., Chen, Z., Huang, C., Liu, W., 2019. Selenium ameliorates AFB 1− induced excess apoptosis in chicken splenocytes through death receptor and endoplasmic reticulum pathways. Biol. Trace Elem. Res. 187, 273–280. https://doi.org/10.1007/s12011-018-1361-7.
FAO, 2013. Mycotoxins. Food safety and quality. Retrieved 01.22.13, from. http://www.fao.org/food/food-safety-quality/a-z-index/mycotoxins/en/.
Gan, F., Xue, H., Huang, Y., Pan, C., Huang, K., 2015b. Selenium alleviates porcine nephrotoxicity of ochratoxin A by improving selenoenzyme expression in vitro. PLoS One 10, e0119808. https://doi.org/10.1371/journal.pone.0119808.
Gan, F., Zhang, Z., Hu, Z., Hesketh, J., Xue, H., Chen, X., Hao, S., Huang, Y., Cole Ezea, P., Parveen, F., Huang, K., 2015a. Ochratoxin A promotes porcine circovirus type 2 replication in vitro and in vivo. Free Radic. Biol. Med. 80, 33–47. https://doi.org/10.1016/j.freeradbiomed.2014.12.016.
Gao, Y., Li, S., Wang, J., Luo, C., Zhao, S., Zheng, N., 2018. Modulation of intestinal epithelial permeability in differentiated Caco-2 cells exposed to aflatoxin M1 and ochratoxin A individually or collectively. Toxins 10, 13. https://doi.org/10.3390/toxins10010013.
Gauthier, T., Duarte-Hospital, C., Vignard, J., Boutet-Robinet, E., Sulyok, M., Snini, S.P., Alassane-Kpembi, I., Lippi, Y., Puel, S., Oswald, I.P., Puel, O., 2020. Versicolorin A, a precursor in aflatoxins biosynthesis, is a food contaminant toxic for human intestinal cells. Environ. Int. 137, 105568 https://doi.org/10.1016/j.envint.2020.105568.
Gémes, B., Takács, E., Gádoros, P., Barócsi, A., Kocsányi, L., Lenk, S., Csákányi, A., Kautny, S., Domján, L., Szarvas, G., Adányi, N., Nabok, A., Mörtl, M., Székács, A., 2021. Development of an immunofluorescence assay module for determination of the mycotoxin zearalenone in water. Toxins 13, 182. https://doi.org/10.3390/toxins13030182.
Gill, S., Kumara, V.M., 2019. Detecting neurodevelopmental toxicity of domoic acid and ochratoxin a using rat fetal neural stem cells. Mar. Drugs 17, 566. https://doi.org/10.3390/md17100566.
Gong, L., Zhu, H., Li, T., Ming, G., Duan, X., Wang, J., Jiang, Y., 2019. Molecular signatures of cytotoxic effects in human embryonic kidney 293 cells treated with single and mixture of ochratoxin A and citrinin. Food Chem. Toxicol. 123, 374–384. https://doi.org/10.1016/j.fct.2018.11.015.
Guan, K., Li, H., Zuo, Z., Wang, F., Hu, P., Peng, X., Fang, J., Cui, H., Shu, G., Ouyang, P., Ouyang, P., 2019. The molecular mechanisms of protective role of Se on the G 0/G 1 phase Arrest caused by AFB 1 in broiler's thymocytes. Biol. Trace Elem. Res. 189, 556–566. https://doi.org/10.1007/s12011-018-1491-y.
Han, Z., Zhang, Y., Wang, C., Liu, X., Jiang, A., Liu, Z., Wang, J., Yang, Z., Wei, Z., 2019. Ochratoxin A-triggered chicken heterophil extracellular traps release through reactive oxygen species production dependent on activation of NADPH oxidase, ERK, and p38 MAPK signaling pathways. J. Agric. Food Chem. 67, 11230–11235. https://doi.org/10.1021/acs.jafc.9b03155.
Heussner, A.H., Bingle, L.E., 2015. Comparative ochratoxin toxicity: a review of the available data. Toxins 7, 4253–4282. https://doi.org/10.3390/toxins7104253.
Hou, L., Gan, F., Zhou, X., Zhou, Y., Qian, G., Liu, Z., Huang, K., 2018. Immunotoxicity of ochratoxin A and aflatoxin B1 in combination is associated with the nuclear factor kappa B signaling pathway in 3D4/21 cells. Chemosphere 199, 718–727. https://doi.org/10.1016/j.chemosphere.2018.02.009.
Hu, P., Zuo, Z., Wang, F., Peng, X., Guan, K., Li, H., Fang, J., Cui, H., Su, G., Ouyang, P., Zhou, Y., 2018b. The protective role of selenium in AFB 1-induced tissue damage and cell cycle arrest in chicken's bursa of fabricius. Biol. Trace Elem. Res. 185, 486–496. https://doi.org/10.1007/s12011-018-1273-6.
Huang, B., Mu, P., Chen, X., Tang, S., Ye, W., Zhu, W., Deng, Y., 2019. Aflatoxin B1 induces S phase arrest by upregulating the expression of p21 via MYC, PLK1 and PLD1. Biochem. Pharmacol. 166, 108–119. https://doi.org/10.1016/j.bcp.2019.05.008.
IARC Working Group on the Evaluation of Carcinogenic Risks to Humans, 2012. Chemical agents and related occupations. IARC Monogr. Eval. Carcinog. Risks Hum. 100 (PT F), 9.
Jahreis, S., Kuhn, S., Madaj, A.M., Bauer, M., Polte, T., 2017. Mold metabolites drive rheumatoid arthritis in mice via promotion of IFN-gamma-and IL-17-producing T cells. Food Chem. Toxicol. 109, 405–413. https://doi.org/10.1016/j.fct.2017.09.027.
Jia, H., Jia, C., An, Q., Cheng, Y., Jiang, X., Xu, Y., Zhao, R., Peng, W., Zhang, Y., Su, J., 2020. Ochratoxin A exposure causes meiotic failure and oocyte deterioration in mice. Theriogenology 148, 236–248. https://doi.org/10.1016/j.theriogenology.2019.11.005.
Jia, X., Cui, J., Meng, X., Xing, L., Shen, H., Wang, J., Liu, J., Wang, Y., Lian, W., Zhang, X., 2016. Malignant transformation of human gastric epithelium cells via reactive oxygen species production and Wnt/β-catenin pathway activation following 40-week exposure to ochratoxin A. Cancer Lett. 372, 36–47. https://doi.org/10.1016/j.canlet.2015.12.007.
Ju, H., Shim, Y., Arumugam, P., Song, J.M., 2016. Crosstalk-eliminated quantitative determination of aflatoxin B1-induced hepatocellular cancer stem cells based on concurrent monitoring of CD133, CD44, and aldehyde dehydrogenase1. Toxicol. Lett. 243, 31–39. https://doi.org/10.1016/j.toxlet.2015.12.006.
Juan-García, A., Tolosa, J., Juan, C., Ruiz, M.J., 2019. Cytotoxicity, genotoxicity and disturbance of cell cycle in HepG2 cells exposed to OTA and BEA: single and combined actions. Toxins 11, 341. https://doi.org/10.3390/toxins11060341.
Khaneghah, A.M., Fakhri, Y., Gahruie, H.H., Niakousari, M., Sant'Ana, A.S., 2019. Mycotoxins in cereal-based products during 24 years (1983–2017): a global systematic review. Trends Food Sci. Technol. 91, 95–105. https://doi.org/10.1016/j.tifs.2019.06.007.
Kim, J., Park, S.H., Do, K.H., Kim, D., Moon, Y., 2016. Interference with mutagenic aflatoxin B1-induced checkpoints through antagonistic action of ochratoxin A in intestinal cancer cells: a molecular explanation on potential risk of crosstalk between carcinogens. Oncotarget 7, 39627. https://doi.org/10.18632/oncotarget.8914.
Kőszegi, T., Poór, M., 2016. Ochratoxin A: molecular interactions, mechanisms of toxicity and prevention at the molecular level. Toxins 8, 111. https://doi.org/10.3390/toxins8040111.
Kousha, K., Thelwall, M., 2008. Sources of google scholar citations outside the science citation index: a comparison between four science disciplines. Scientometrics 74, 273–294. https://doi.org/10.1007/s11192-008-0217-x.
Kovalsky, P., Kos, G., Nährer, K., Schwab, C., Jenkins, T., Schatzmayr, G., Sulyok, M., Krska, R., 2016. Co- occurrence of regulated, masked and emerging mycotoxins and secondary metabo- lites in finished feed and maize—an extensive survey. Toxins 8, 363. https://doi.org/10.3390/toxins8120363.
Kumar, P., Mahato, D.K., Kamle, M., Mohanta, T.K., Kang, S.G., 2017. Aflatoxins: a global concern for food safety, human health and their management. Front. Microbiol. 7, 2170. https://doi.org/10.3389/fmicb.2016.02170.
Kupski, L., Freitas, M., Ribeiro, D., Furlong, E.B., Fernandes, E., 2016. Ochratoxin A activates neutrophils and kills these cells through necrosis, an effect eliminated through its conversion into ochratoxin α. Toxicology 368, 91–102. https://doi.org/10.1016/j.tox.2016.09.001.
Kutsanedzie, F.Y., Agyekum, A.A., Annavaram, V., Chen, Q., 2020. Signal-enhanced SERS-sensors of CAR-PLS and GA-PLS coupled AgNPs for ochratoxin A and aflatoxin B1 detection. Food Chem. 315, 126231 https://doi.org/10.1016/j.foodchem.2020.126231.
Lan, M., Zhang, Y., Wan, X., Pan, M.H., Xu, Y., Sun, S.C., 2020. Melatonin ameliorates ochratoxin A-induced oxidative stress and apoptosis in porcine oocytes. Environ. Pollut. 256, 113374 https://doi.org/10.1016/j.envpol.2019.113374.
Le, G., Yuan, X., Hou, L., Ge, L., Liu, S., Muhmood, A., Li, K., Lin, Z., Liu, D., Gan, F., Song, S., Pan, C., Chen, X., Huang, K., 2020. Ochratoxin A induces glomerular injury through activating the ERK/NF-κB signaling pathway. Food Chem. Toxicol. 143, 111516 https://doi.org/10.1016/j.fct.2020.111516.
Leitão, A.L., 2019. Occurrence of ochratoxin A in coffee: Threads and solutions—a mini-review. Beverages 5, 36. https://doi.org/10.3390/beverages5020036.
Li, H., Li, S., Yang, H., Wang, Y., Wang, J., Zheng, N., 2019. l-Proline alleviates kidney injury caused by AFB1 and AFM1 through regulating excessive apoptosis of kidney cells. Toxins 11, 226. https://doi.org/10.3390/toxins11040226.
Li, H., Malyar, R.M., Zhai, N., Wang, H., Liu, K., Liu, D., Pan, C., Gan, F., Huang, K., Miao, J., Chen, X., 2019. Zinc supplementation alleviates OTA-induced oxidative stress and apoptosis in MDCK cells by up-regulating metallothioneins. Life Sci. 234, 116735 https://doi.org/10.1016/j.lfs.2019.116735.
Li, H., Mao, X., Liu, K., Sun, J., Li, B., Malyar, R.M., Liu, D., Pan, C., Gan, F., Liu, Y., Huang, K., Chen, X., 2021. Ochratoxin A induces nephrotoxicity in vitro and in vivo via pyroptosis. Arch. Toxicol. 95, 1489–1502. https://doi.org/10.1007/s00204-021-02993-6.

Liang, R., Shen, X.L., Zhang, B., Li, Y., Xu, W., Zhao, C., Luo, Y., Huang, K., 2015. Apoptosis signal-regulating kinase 1 promotes Ochratoxin A-induced renal cytotoxicity. Sci. Rep. 5, 1–12. https://doi.org/10.1038/srep08078.

Liu, C., Jiang, M., Fang, J., Peng, X.I., Cui, H., 2016. Inhibitory effects of dietary aflatoxin B1 on cytokines expression and T-cell subsets in the cecal tonsil of broiler chickens. Spanish J. Agric. Res. 14, 10. https://doi.org/10.5424/sjar/2016143-8811.

Liu, D., Su, J., Lin, J., Qian, G., Chen, X., Song, S., Huang, K., 2018. Activation of AMPK-dependent SIRT-1 by astragalus polysaccharide protects against ochratoxin A-induced immune stress in vitro and in vivo. Int. J. Biol. Macromol. 120, 683–692. https://doi.org/10.1016/j.ijbiomac.2018.08.156.

Liu, J., Wu, S., Shen, H., Cui, J., Wang, Y., Xing, L., Wang, J., Yan, X., Zhang, X., 2015. Ochratoxin A induces DNA damage and G2 phase arrest in human esophageal epithelium Het-1A cells in vitro. J. Toxicol. Sci. 40, 657–665. https://doi.org/10.2131/jts.40.657.

Liu, K., Mao, X., Li, H., Liu, D., Le, G., Gan, F., Pan, C., Huang, K., Chen, X., 2020. Regulation of taurine in OTA-induced apoptosis and autophagy. Toxicon 181, 82–90. https://doi.org/10.1016/j.toxicon.2020.04.097.

Liu, Y., Wang, W., 2016. Aflatoxin B1 impairs mitochondrial functions, activates ROS generation, induces apoptosis and involves Nrf2 signal pathway in primary broiler hepatocytes. Anim. Sci. J. 87, 1490–1500. https://doi.org/10.1111/asj.12550.

Loboda, A., Stachurska, A., Podkalicka, P., Sobczak, M., Mucha, O., Witalisz-Siepracka, A., Jozkowicz, A., Dulak, J., 2017. Effect of heme oxygenase-1 on ochratoxin A-induced nephrotoxicity in mice. J. Bioche. Cell Biol. 84, 46–57. https://doi.org/10.1016/j.biocel.2017.01.003.

Luo, Y., Liu, X., Li, J., 2018. Updating techniques on controlling mycotoxins-A review. Food Control 89, 123–132. https://doi.org/10.1016/j.foodcont.2018.01.016.

Luz, C., Ferrer, J., Mañes, J., Meca, G., 2018. Toxicity reduction of ochratoxin A by lactic acid bacteria. Food Chem. Toxicol. 112, 60–66. https://doi.org/10.1016/j.fct.2017.12.030.

Malir, F., Ostry, V., Pfohl-Leszkowicz, A., Malir, J., Toman, J., 2016. Ochratoxin A: 50 years of research. Toxins 8, 191. https://doi.org/10.3390/toxins8070191.

Martín-Martín, A., Thelwall, M., Orduna-Malea, E., López-Cózar, E.D., 2021. Google scholar, Microsoft academic, Scopus, dimensions, Web of science, and OpenCitations' COCI: a multidisciplinary comparison of coverage via citations. Scientometrics 126, 871–906. https://doi.org/10.1007/s11192-020-03690-4.

Mehrzad, J., Bahari, A., Bassami, M.R., Mahmoudi, M., Dehghani, H., 2018a. Data on environmentally relevant level of aflatoxin B1-induced human dendritic cells' functional alteration. Data Brief 18, 1576–1580. https://doi.org/10.1016/j.dib.2018.04.104.

Mehrzad, J., Fazel, F., Pouyamehr, N., Hosseinkhani, S., Dehghani, H., 2020. Naturally occurring level of aflatoxin B1 injures human, canine and bovine leukocytes through ATP depletion and caspase activation. Int. J. Toxicol. 39, 30–38. https://doi.org/10.1177/1091581819892613.

Mehrzad, J., Hosseinkhani, S., Malvandi, A.M., 2018b. Human microglial cells undergo proapoptotic induction and inflammatory activation upon in vitro exposure to a naturally occurring level of aflatoxin B1. Neuroimmunomodulation 25, 176–183. https://doi.org/10.1159/000493528.

Nakayama, H., Kitagawa, N., Otani, T., Iida, H., Anan, H., Inai, T., 2018. Ochratoxin A, citrinin and deoxynivalenol decrease claudin-2 expression in mouse rectum CMT93-II cells. Microscopy 67, 99–111. https://doi.org/10.1093/jmicro/dfy005.

Nguyen, N.T., Varga, E., Maragos, C., Baumgartner, S., Adam, G., Berthiller, F., 2019. Cross-reactivity of commercial and non-commercial deoxynivalenol-antibodies to emerging trichothecenes and common deoxynivalenol-derivatives. World Mycotoxin J. 12, 45–53. https://doi.org/10.3920/WMJ2018.2363.

Niaz, K., Shah, S.Z.A., Khan, F., Bule, M., 2020. Ochratoxin A–induced genotoxic and epigenetic mechanisms lead to Alzheimer disease: its modulation with strategies. Environ. Sci. Pollut. Res. 27, 44673–44700. https://doi.org/10.1007/s11356-020-08991-y.

Nones, J., Solhaug, A., Eriksen, G.S., Macuvele, D.L.P., Poli, A., Soares, C., Trentin, A.G., Riella, H.G., Nones, J., 2017. Bentonite modified with zinc enhances aflatoxin B1 adsorption and increase survival of fibroblasts (3T3) and epithelial colorectal adenocarcinoma cells (Caco-2). J. Hazard Mater. 337, 80–89. https://doi.org/10.1016/j.jhazmat.2017.04.068.

Oskoueian, E., Abdullah, N., Zulkifli, I., Ebrahimi, M., Karimi, E., Goh, Y.M., Oskoueian, A., Shakeri, M., 2015. Cytoprotective effect of palm kernel cake phenolics against aflatoxin B1-induced cell damage and its underlying mechanism of action. BMC Compl. Alternative Med. 15, 1–12. https://doi.org/10.1186/s12906-015-0921-z.

Ostry, V., Malir, F., Toman, J., Grosse, Y., 2017. Mycotoxins as human carcinogens—the IARC Monographs classification. Mycotoxin Res. 33, 65–73. https://doi.org/10.1007/s12550-016-0265-7.

Paradells, S., Rocamonde, B., Llinares, C., Herranz-Pérez, V., Jimenez, M., Garcia-Verdugo, J.M., Zipancic, I., Soria, J.M., Garcia-Esparza, M.A., 2015. Neurotoxic effects of ochratoxin A on the subventricular zone of adult mouse brain. J. Appl. Toxicol. 35, 737–751. https://doi.org/10.1002/jat.3061.

Park, H., Park, H.S., Lim, W., Song, G., 2020. Ochratoxin A suppresses proliferation of Sertoli and Leydig cells in mice. Med. Mycol. J. 58, 71–82. https://doi.org/10.1093/mmy/myz016.

Park, S., Lim, W., You, S., Song, G., 2019. Ochratoxin A exerts neurotoxicity in human astrocytes through mitochondria-dependent apoptosis and intracellular calcium overload. Toxicol. Lett. 313, 42–49. https://doi.org/10.1016/j.toxlet.2019.05.021.

Peng, X., Bai, S., Ding, X., Zhang, K., 2017. Pathological impairment, cell cycle arrest and apoptosis of thymus and bursa of fabricius induced by aflatoxin-contaminated corn in Broilers. Int. J. Environ. Res. Publ. Health 14, 77. https://doi.org/10.3390/ijerph14010077.

Peng, X., Bai, S., Ding, X., Zeng, Q., Zhang, K., Fang, J., 2015. Pathological changes in the immune organs of broiler chickens fed on corn naturally contaminated with aflatoxins B1 and B2. Avian Pathol. 44, 192–199. https://doi.org/10.1080/03079457.2015.1023179.

Peng, X., Chen, K., Chen, J., Fang, J., Cui, H., Zuo, Z., Deng, J., Chen, Z., Geng, Y., Lai, W., Lai, W., 2016. Aflatoxin B 1 affects apoptosis and expression of B ax, B cl-2, and Caspase-3 in thymus and bursa of fabricius in broiler chickens. Environ. Toxicol. 31, 1113–1120. https://doi.org/10.1002/tox.22120.

Qi, X., Zhu, L., Yang, B., Luo, H., Xu, W., He, X., Huang, K., 2018. Mitigation of cell apoptosis induced by ochratoxin A (OTA) is possibly through organic cation transport 2 (OCT2) knockout. Food Chem. Toxicol. 121, 15–23. https://doi.org/10.1016/j.fct.2018.08.026.

Qian, G., Liu, D., Hu, J., Gan, F., Hou, L., Chen, X., Huang, K., 2017. Ochratoxin A-induced autophagy in vitro and in vivo promotes porcine circovirus type 2 replication. Cell Death Dis. 8 https://doi.org/10.1038/cddis.2017.303 e2909-e2909.

Qian, G., Liu, D., Hu, J., Gan, F., Hou, L., Zhai, N., Chen, X., Huang, K., 2018. SeMet attenuates OTA-induced PCV2 replication promotion by inhibiting autophagy by activating the AKT/mTOR signaling pathway. Vet. Res. 49, 1–12. https://doi.org/10.1186/s13567-018-0508-z.

Qiu, T., Shen, X., Tian, Z., Huang, R., Li, X., Wang, J., Sun, Y., Jiang, Y., Lei, H., Zhang, H., 2018. IgY reduces AFB1-Induced cytotoxicity, cellular dysfunction, and genotoxicity in human L-02 hepatocytes and swan 71 trophoblasts. J. Agric. Food Chem. 66, 1543–1550. https://doi.org/10.1021/acs.jafc.7b05385.

Qureshi, H., Hamid, S.S., Ali, S.S., Anwar, J., Siddiqui, A.A., Khan, N.A., 2015. Cytotoxic effects of aflatoxin B1 on human brain microvascular endothelial cells of the blood-brain barrier. Med. Mycol. 53, 409–416. https://doi.org/10.1093/mmy/myv010.

Ráduly, Z., Szabó, L., Madar, A., Pócsi, I., Csernoch, L., 2020. Toxicological and medical aspects of Aspergillus-derived mycotoxins entering the feed and food chain. Front. Microbiol. 10, 2908. https://doi.org/10.3389/fmicb.2019.02908.

Raghubeer, S., Nagiah, S., Phulukdaree, A., Chuturgoon, A., 2015. The phytoalexin resveratrol ameliorates ochratoxin A toxicity in human embryonic kidney (HEK293) cells. J. Cell. Biochem. 116, 2947–2955. https://doi.org/10.1002/jcb.25242.

Ricci, F.G., Terkelli, L.R., Venancio, E.J., Justino, L., Dos Santos, B.Q., Baptista, A.A.S., Oba, A., de Oliveira Souza, B.D., Bracarense, A.P.F.R.L., Hirooka, E.Y., Itano, E.N., 2021. Tryptophan attenuates the effects of OTA on intestinal morphology and local IgA/IgY production in broiler chicks. Toxins 13, 5. https://doi.org/10.3390/toxins13010005.

Rushing, B.R., Selim, M.I., 2019. Aflatoxin B1: a review on metabolism, toxicity, occurrence in food, occupational exposure, and detoxification methods. Food Chem. Toxicol. 124, 81–100. https://doi.org/10.1016/j.fct.2018.11.047.

Sali, N., Nagy, S., Poór, M., Kőszegi, T., 2016. Multiparametric luminescent cell viability assay in toxicology models: a critical evaluation. J. Pharmacol. Toxicol. Methods 79, 45–54. https://doi.org/10.1016/j.vascn.2016.01.004.

Sánchez-Montero, L., Córdoba, J.J., Alía, A., Peromingo, B., Núñez, F., 2019. Effect of Spanish smoked paprika "Pimentón de La Vera" on control of ochratoxin A and aflatoxins production on a dry-cured meat model system. Int. J. Food Microbiol. 308, 108303 https://doi.org/10.1016/j.ijfoodmicro.2019.108303.

Sarma, U.P., Bhetaria, P.J., Devi, P., Varma, A., 2017. Aflatoxins: implications on health. Indian J. Clin. Biochem. 32, 124–133. https://doi.org/10.1007/s12291-017-0649-2.

Sarmast, E., Fallah, A.A., Jafari, T., Khaneghah, A.M., 2020. Occurrence and fate of mycotoxins in cereals and cereal-based products: a narrative review of systematic reviews and meta-analyses studies. Curr. Opin. Food Sci. https://doi.org/10.1016/j.cofs.2020.12.013.

Shen, Y., Shi, Z., Fan, J.T., Yan, B., 2020. Dechlorination and demethylation of ochratoxin A enhance blocking activity of PXR activation, suppress PXR expression and reduce cytotoxicity. Toxicol. Lett. 332, 171–180. https://doi.org/10.1016/j.toxlet.2020.07.012.

Shin, K.T., Guo, J., Niu, Y.J., Cui, X.S., 2018. The toxic effect of aflatoxin B1 on early porcine embryonic development. Theriogenology 118, 157–163. https://doi.org/10.1016/j.theriogenology.2018.06.002.

Singh, A.K., Lakshmi, G.B.V.S., Fernandes, M., Sarkar, T., Gulati, P., Singh, R.P., Solanki, P.R., 2021. A simple detection platform based on molecularly imprinted polymer for AFB1 and FuB1 mycotoxins. Microchem. J. 171, 106730 https://doi.org/10.1016/j.microc.2021.106730.

Soler, L., Oswald, I.P., 2018. The importance of accounting for sex in the search of proteomic signatures of mycotoxin exposure. J. Proteome 178, 114–122. https://doi.org/10.1016/j.jprot.2017.12.017.

Streit, E., Naehrer, K., Rodrigues, I., Schatzmayr, G., 2013. Mycotoxin occurrence in feed and feed raw materials worldwide: long-term analysis with special focus on Europe and Asia. J. Sci. Food Agric. 93, 2892–2899. https://doi.org/10.1002/jsfa.6225.

Su, Z., Ye, X., Peng, T., Xiao, K., Shang, L., 2017. Aflatoxin B1 damages peripheral blood lymphocytes in patients with primary hepatocellular carcinoma by inducing peroxidation. Int. J. Clin. Exp. Med. 10, 13703–13709.

Sun, Y., Liu, Z., Liu, D., Chen, J., Gan, F., Huang, K., 2018. Low-level aflatoxin B1 promotes influenza infection and modulates a switch in macrophage polarization from M1 to M2. Cell. Physiol. Biochem. 49, 1151–1167. https://doi.org/10.1159/000493294.

Tao, Y., Xie, S., Xu, F., Liu, A., Wang, Y., Chen, D., Pan, Y., Huang, L., Peng, D., Wang, X., Yuan, Z., 2018. Ochratoxin A: toxicity, oxidative stress and metabolism. Food Chem. Toxicol. 112, 320–331. https://doi.org/10.1016/j.fct.2018.01.002.

Topi, D., Babič, J., Pavšič-Vrtač, K., Tavčar-Kalcher, G., Jakovac-Strajn, B., 2021. Incidence of Fusarium mycotoxins in wheat and maize from Albania. Molecules 26, 172. https://doi.org/10.3390/molecules26010172.

Umesha, S., Manukumar, H.M.G., Chandrasekhar, B., Shivakumara, P., Shiva Kumar, J., Raghava, S., Avinash, P., Shirin, M., Bharathi, T.R., Rajini, S.B., Nandhini, M., Vinaya Rani, G.G., Shobha, M., Prakash, H.S., 2017. Aflatoxins and food pathogens:

impact of biologically active aflatoxins and their control strategies. J. Sci. Food Agric. 97, 1698–1707. https://doi.org/10.1002/jsfa.8144.
Vahidi-Ferdowsi, P., Mehrzad, J., Malvandi, A.M., Hosseinkhani, S., 2018. Bioluminescence-based detection of astrocytes apoptosis and ATP depletion induced by biologically relevant level aflatoxin B1. World Mycotoxin J. 11, 589–598. https://doi.org/10.3920/WMJ2017.2275.
Wang, H., Chen, Y., Zhai, N., Chen, X., Gan, F., Li, H., Huang, K., 2017. Ochratoxin A-induced apoptosis of IPEC-J2 cells through ROS-mediated mitochondrial permeability transition pore opening pathway. J. Agric. Food Chem. 65, 10630–10637. https://doi.org/10.1021/acs.jafc.7b04434.
Wang, H., Li, H., Chen, X., Huang, K., 2018. ERK1/2-mediated autophagy is essential for cell survival under Ochratoxin A exposure in IPEC-J2 cells. Toxicol. Appl. Pharmacol. 360, 38–44. https://doi.org/10.1016/j.taap.2018.09.027.
Wang, H., Wei, Y., Xie, Y., Yan, C., Du, H., Li, Z., 2020. Ochratoxin A and fumonisin B1 exhibit synergistic cytotoxic effects by inducing apoptosis on rat liver cells. Toxicon 181, 19–27. https://doi.org/10.1016/j.toxicon.2020.04.094.
Wu, B., Mughal, M.J., Fang, J., Peng, X., 2019. The protective role of selenium against AFB 1-induced liver apoptosis by death receptor pathway in broilers. Biol. Trace Elem. Res. 191, 453–463. https://doi.org/10.1007/s12011-018-1623-4.
Wu, K., Jia, S., Zhang, J., Zhang, C., Wang, S., Rajput, S.A., Sun, L., Qi, D., 2021. Transcriptomics and flow cytometry reveals the cytotoxicity of aflatoxin B1 and aflatoxin M1 in bovine mammary epithelial cells. Ecotoxicol. Environ. Saf. 209, 111823 https://doi.org/10.1016/j.ecoenv.2020.111823.
Xu, H., Hao, S., Gan, F., Wang, H., Xu, J., Liu, D., Huang, K., 2017. In vitro immune toxicity of ochratoxin A in porcine alveolar macrophages: a role for the ROS-relative TLR4/MyD88 signaling pathway. Chem. Biol. Interact. 272, 107–116. https://doi.org/10.1016/j.cbi.2017.05.016.
Xu, Q., Shi, W., Lv, P., Meng, W., Mao, G., Gong, C., Chen, Y., Wei, Y., He, X., Zhao, J., Han, H., Sun, M., Xiao, K., 2020. Critical role of caveolin-1 in aflatoxin B1-induced hepatotoxicity via the regulation of oxidation and autophagy. Cell Death Dis. 11, 1–16. https://doi.org/10.1038/s41419-019-2197-6.
Yang, X., Li, Y., Zheng, L., He, X., Luo, Y., Huang, K., Xu, W., 2019. Glucose-regulated protein 75 in foodborne disease models induces renal tubular necrosis. Food Chem. Toxicol. 133, 110720 https://doi.org/10.1016/j.fct.2019.110720.
Yang, X., Lv, Y., Huang, K., Luo, Y., Xu, W., 2016. Zinc inhibits aflatoxin B1-induced cytotoxicity and genotoxicity in human hepatocytes (HepG2 cells). Food Chem. Toxicol. 92, 17–25. https://doi.org/10.1016/j.fct.2016.03.012.
Yin, H., Jiang, M., Peng, X., Cui, H., Zhou, Y., He, M., Zuo, Z., Ouyang, P., Fan, J., Fang, J., 2016. The molecular mechanism of G2/M cell cycle arrest induced by AFB1 in the jejunum. Oncotarget 7, 35592. https://doi.org/10.18632/oncotarget.9594.
Ying, C., Hong, W., Nianhui, Z., Chunlei, W., Kehe, H., Cuiling, P., 2019. Nontoxic concentrations of OTA aggravate DON-induced intestinal barrier dysfunction in IPEC-J2 cells via activation of NF-κB signaling pathway. Toxicol. Lett. 311, 114–124. https://doi.org/10.1016/j.toxlet.2019.04.021.
Yu, Z., Wang, F., Liang, N., Wang, C., Peng, X., Fang, J., Cui, H., Jameel Mughal, M., Lai, W., 2015. Effect of selenium supplementation on apoptosis and cell cycle blockage of renal cells in broilers fed a diet containing aflatoxin B 1. Biol. Trace Elem. Res. 168 (1), 242–251. https://doi.org/10.1007/s12011-015-0344-1.
Yu, Z., Wu, F., Tian, J., Guo, X., An, R., 2018. Protective effects of compound ammonium glycyrrhizin, L-arginine, silymarin and glucurolactone against liver damage induced by ochratoxin A in primary chicken hepatocytes. Mol. Med. Rep. 18, 2551–2560. https://doi.org/10.3892/mmr.2018.9285.
Zhai, N., Wang, H., Chen, Y., Li, H., Viktor, K., Huang, K., Chen, X., 2018. Taurine attenuates OTA-promoted PCV2 replication through blocking ROS-dependent autophagy via inhibiting AMPK/mTOR signaling pathway. Chem. Biol. Int. 296, 220–228. https://doi.org/10.1016/j.cbi.2018.10.005.
Zhang, B., Zhu, L., Dai, Y., Li, H., Huang, K., Luo, Y., Xu, W., 2020. An in vitro attempt at precision toxicology reveals the involvement of DNA methylation alteration in ochratoxin A-induced G0/G1 phase arrest. Epigenetics 15, 199–214. https://doi.org/10.1080/15592294.2019.1644878.
Zhang, L.Y., Zhan, D.L., Chen, Y.Y., Wang, W.H., He, C.Y., Lin, Y., Lin, Y.C., Lin, Z.N., 2019. Aflatoxin B1 enhances pyroptosis of hepatocytes and activation of Kupffer cells to promote liver inflammatory injury via dephosphorylation of cyclooxygenase-2: an in vitro, ex vivo and in vivo study. Arch. Toxicol. 93, 3305–3320. https://doi.org/10.1007/s00204-019-02572-w.
Zhang, T.Y., Wu, R.Y., Zhao, Y., Xu, C.S., Zhang, W.D., Ge, W., Liu, J., Sun, Z.Y., Zou, S. H., Shen, W., 2018. Ochratoxin A exposure decreased sperm motility via the AMPK and PTEN signaling pathways. Toxicol. Appl. Pharmacol. 340, 49–57. https://doi.org/10.1016/j.taap.2017.12.011.
Zhao, T., Shen, X.L., Chen, W., Liao, X., Yang, J., Wang, Y., Zou, Y., Fang, C., 2017. Advances in research of nephrotoxicity and toxic antagonism of ochratoxin A. Toxin Rev. 36, 39–44. https://doi.org/10.1080/15569543.2016.1243560.
Zheng, Z., Zuo, Z., Zhu, P., Wang, F., Yin, H., Peng, X., Fang, J., Cui, H., Gao, C., Song, H., Ouyang, P., Zhou, Y., Zhao, S., 2017. A study on the expression of apoptotic molecules related to death receptor and endoplasmic reticulum pathways in the jejunum of AFB1-intoxicated chickens. Oncotarget 8, 89655. https://doi.org/10.18632/oncotarget.20333.
Zhou, X., Gan, F., Hou, L., Liu, Z., Su, J., Lin, Z., Le, G., Huang, K., 2019. Aflatoxin B1 induces immunotoxicity through the DNA methyltransferase-mediated JAK2/STAT3 pathway in 3D4/21 cells. J. Agric. Food Chem. 67, 3772–3780. https://doi.org/10.1021/acs.jafc.8b07309.
Zhou, Y., Wu, S., Wang, F., Li, Q., He, C., Duan, N., Wang, Z., 2020. Assessing the toxicity in vitro of degradation products from deoxynivalenol photocatalytic degradation by using upconversion nanoparticles@ TiO2 composite. Chemosphere 238, 124648. https://doi.org/10.1016/j.chemosphere.2019.124648.
Zhu, L., Yu, T., Qi, X., Yang, B., Shi, L., Luo, H., He, X., Huang, K., Xu, W., 2016. miR-122 plays an important role in ochratoxin A-induced hepatocyte apoptosis in vitro and in vivo. Toxicol. Res. 5, 160–167. https://doi.org/10.1039/c5tx00104h.
Zhu, L., Zhang, B., Dai, Y., Li, H., Xu, W., 2017. A review: epigenetic mechanism in ochratoxin A toxicity studies. Toxins 9 (4), 113. https://doi.org/10.3390/toxins9040113.